COO-1198-500

THE THIRD ORDER ELASTIC CONSTANTS OF ALUMINUM

Joseph F. Thomas, Jr.

Department of Physics and Materials Research Laboratory

University of Illinois, Urbana, Illinois

February 1968

This is a technical information document based on a thesis submitted by Joseph F. Thomas, Jr., in partial fulfillment of the requirements for the degree of Doctor of Philosophy in Physics in the Graduate College of the University of Illinois, 1968. The research was supported by the U. S. Atomic Energy Commission under Contract AT(11-1)-1198.

DISCLAIMER

COO-1198-500

THE THIRD ORDER ELASTIC CONSTANTS OF ALUMINUM

Joseph F. Thomas, Jr.

Department of Physics and Materials Research Laboratory

University of Illinois, Urbana, Illinois

February 1968

This is a technical information document based on a thesis submitted by Joseph F. Thomas, Jr., in partial fulfillment of the requirements for the degree of Doctor of Philosophy in Physics in the Graduate College of the University of Illinois, 1968. The research was supported by the U. S. Atomic Energy Commission under Contract AT(11-1)-1198.

THE THIRD ORDER ELASTIC CONSTANTS OF ALUMINUM

Joseph Francis Thomas, Jr., Ph.D.
Department of Physics
University of Illinois, 1968

The complete set of six third order elastic constants of single crystal Al has been experimentally determined by measuring both hydrostatic pressure and uniaxial stress derivatives of the natural sound velocities using a two specimen interferometric technique. The values obtained are

$C_{111} = -10.76$ $\quad C_{144} = -0.23$

$C_{112} = -3.15$ $\quad C_{166} = -3.40$

$C_{123} = +0.36$ $\quad C_{456} = -0.30$

in units of 10^{12} dyn.cm^{-2}. The specimens were neutron irradiated to eliminate dislocation effects from the uniaxial experiments. A self-consistent set of hydrostatic pressure derivatives of the second order elastic constants has been calculated from the measured third order elastic constants. The third order elastic constants have also been used to calculate the thermal expansion in the anisotropic continuum model at both high and low temperatures, and a comparison has been made to the directly measured expansion coefficients.

The seven independent relations between second and third order elastic constants and appropriate lattice energy derivatives in a Fuchs approach have been obtained. The related deformation parameters have been described in a consistent fashion. The applicability of the Fuchs approach to elastic constant calculations for metal crystals has been discussed in terms of the neglect of energy terms which depend upon volume only.

An attempt has been made to calculate the second and third order elastic constants of Al in a Fuchs approach using a Wigner-Seitz decomposition of the lattice energy. The terms considered were the electrostatic energy and the Fermi energy. The Fermi energy was treated in a nearly-free-electron approximation. The fact that this attempt was unsuccessful has been attributed to the complicated energy band structure of Al in the vicinity of the Brillouin zone boundaries.

ACKNOWLEDGMENTS

The author wishes to express his gratitude for the guidance and encouragement of his advisor, Prof. A. V. Granato.

He would also like to thank Prof. Y. Hiki for introducing him to the experimental techniques, Prof. T. Suzuki for many extremely enlightening discussions concerning the calculation of elastic constants, and Prof. N. W. Ashcroft for a particularly helpful discussion of the Fermi surface of Al.

He is also indebted to Mr. T. L. Ochs for his skillful assistance with the sample preparation, and to Messrs. Ochs, W. S. deRosset, and R. O. Schwenker for assistance in conducting the experiments.

The support of the United States Atomic Energy Commission is gratefully acknowledged.

TABLE OF CONTENTS

LIST OF TABLES

Table | Page

LIST OF FIGURES

I. INTRODUCTION

The mechanical and thermal properties of a crystalline solid are intimately related to the form of the lattice potential energy. It will be useful to consider the general aspects of this relationship.

Several mechanical and thermal properties can be adequately described in the harmonic approximation. In this approximation, infinitesimal lattice movements can be expressed in terms of a set of normal modes of lattice vibration. Static deformations will obey Hooke's law; sound wave propagation can be described by the elastic wave equation; and the lattice heat capacity can be calculated at moderate temperatures. The harmonic model, however, will not account for many well known mechanical and thermal properties. There will be no thermal expansion; insulators will have no thermal resistance; and sound waves will not be attenuated.

These properties are related to the anharmonic nature of the lattice potential energy. In an anharmonic model, lattice movements must be described in terms of interacting modes of vibration. Large static deformations will deviate from Hooke's law; sound waves will interact with each other and with the thermal vibrations of the lattice; and the lattice will expand with a change in temperature.

A full anharmonic model is capable of describing all mechanical and thermal properties of a perfect crystal. The problem reduces to one of calculation rather than one of formulation. In the usual approach of a discrete lattice dynamics, one obtains a model expressed in terms of a large number of parameters generally referred to as force constants. There are several difficulties in obtaining numerical results from such an approach. In general, the parameters are too numerous to be determined directly by experiment. In many cases, particularly in the study

of metals, the force constants also lack a clear physical interpretation in terms of the cohesive properties of the crystal.

An alternative approach is to utilize the finite deformation theory of an elastic continuum. The change in the lattice potential energy associated with deformation away from an equilibrium configuration can be expressed as a power series in an elastic strain parameter. The coefficients in such an expansion are elastic constants. The coefficient of an n^{th} order term in the strain parameter is called an n^{th} order elastic constant. It follows that the second order elastic constants are the usual elastic constants relating stress to strain in Hooke's law. The higher order elastic constants, which are clearly related to deviations from Hooke's law, provide an efficient measure of many aspects of the lattice anharmonicity.

This can be clarified by considering a simple, one-dimensional model. For a one-dimensional solid, a convenient strain parameter would be the deviation of the particle separation from the equilibrium separation, $(r-r_o)$. In a harmonic model, the energy per particle would be a quadratic function of this strain parameter,

$$E = E_o + \tfrac{1}{2}k(r-r_o)^2 \quad . \qquad (1)$$

To examine the anharmonic nature of the energy, however, we need a more realistic energy function. A basic measure of the anharmonicity is the asymmetry of the lattice energy with respect to particle separation. We can modify Eq. (1) by simply adding a term which is not symmetric about $r = r_o$. For example, we can write

$$E = E_o + \frac{1}{2}k(r-r_o)^2 - \frac{1}{6}g(r-r_o)^3 \quad . \qquad (2)$$

For this model the usual elastic constant could be written as

$$C_2 = \frac{d^2E}{d(r-r_o)^2} = k - g(r-r_o) \ . \qquad (3)$$

We see that as the chain is compressed, $r < r_o$, the elastic constant will increase. Correspondingly, for a real solid, the usual elastic constants are functions of pressure, and the pressure derivatives are usually positive.

An alternative description would be to define a second order elastic constant as a second energy derivative evaluated at equilibrium particle separation,

$$C_2^o = \left.\frac{d^2E}{d(r-r_o)^2}\right|_{r=r_o} = k \ . \qquad (4)$$

To describe the mechanical and thermal behavior of this one-dimensional solid, we would then need the higher order elastic constants. In particular, the third order elastic constant would be

$$C_3^o = \left.\frac{d^3E}{d(r-r_o)^3}\right|_{r=r_o} = -g \ , \qquad (5)$$

and the elastic constants of still higher order would be identically zero.

The formalism for a real, three-dimensional solid is quite analogous to this simple model. We define the vector displacement $\underline{u}$ of a particle from an initial coordinate $\underline{a}$ to a final coordinate $\underline{r}$,

$$\underline{u} = \underline{r} - \underline{a} \ . \qquad (6)$$

It is most convenient to work with the finite Lagrangian strain tensor which is defined as[1]

$$\eta_{ij} = \tfrac{1}{2}\left[\frac{\partial u_i}{\partial a_j} + \frac{\partial u_j}{\partial a_i} + \frac{\partial u_k}{\partial a_i} \frac{\partial u_k}{\partial a_j} \right] . \tag{7}$$

Here u_i etc. indicates the i^{th} cartesian component of the vector $\underline{u}$, and repeated indices are always to be summed over. Equation (7) describes exactly relative displacements in the solid, eliminating the effect of rigid body rotations. The description is exact in the following terms: If $\delta\underline{a}$ is the initial separation of two particles in the solid, and $\delta\underline{r}$ is the final separation after a deformation has been applied, then

$$(\delta\underline{r})^2 - (\delta\underline{a})^2 = 2\eta_{ij}\, \delta a_i\, \delta a_j . \tag{8}$$

In describing the thermodynamic properties of the deformed lattice, we can work with either the internal energy per unit mass $U(\underline{r},S)$ or the Helmholtz free energy per unit mass $F(\underline{r},T)$. Here S and T are, respectively, the entropy and the temperature. Elastic constants of any order can then be defined as the expansion coefficients of U (or F) in terms of the Lagrangian strain tensor components.[2] More exactly,

$$C^S_{ijklmn..} = \rho_o \left[\frac{\partial^n U}{\partial\eta_{ij}\, \partial\eta_{kl}\, \partial\eta_{mn..}} \right]_{S,\eta = 0}$$

$$C^T_{ijklmn..} = \rho_o \left[\frac{\partial^n F}{\partial\eta_{ij}\, \partial\eta_{kl}\, \partial\eta_{mn..}} \right]_{T,\eta = 0} \tag{9}$$

Here superscript S indicates an adiabatic elastic constant which must be used to describe an isentropic process. Similarly, superscript T indicates an isothermal elastic constant which must be used to describe an isothermal process.

The elastic constants of Eq. (9) represent the solid in configuration $\underline{a}$. If the coordinates $\underline{a}$ represent the natural, unstressed configuration of a solid, then the $C_{ijklmn..}$ are those elastic constants which would be calculated from atomic models of the lattice energy. If the coordinates $\underline{a}$ represent a stressed configuration of the solid, then the $C_{ijklmn..}$ are related simply to the applied stress and the elastic coefficient which would be measured experimentally. These relationships have recently been clearly summarized by Wallace.[3]

We note that the second order elastic constants are elements of a fourth rank tensor which has, in general, 81 independent components. However, it is well known that for a cubic crystal, which we are primarily interested in here, symmetry considerations reduce this number to three. The third order elastic constants are elements of a sixth rank tensor with, in general, 729 independent components. For cubic crystals, however, symmetry considerations will reduce this number to six. These six numbers can be measured experimentally and, in addition, can be made physically meaningful in terms of the energy change during a particular deformation. The third order elastic constants will provide a convenient description of many anharmonic properties of a crystalline solid.

Measurements of third order elastic constants have been reported for approximately ten single crystal materials including semiconductors, piezoelectrics, alkali halides, and, more recently, metals. An extensive literature on the subject has developed during the past six years. A complete review will not be attempted here. Rather, we shall concentrate on measurements on metal single crystals.

The most powerful method for obtaining anharmonic data in the continuum model is the measurement of sound velocity changes with

applied homogeneous stress. Basic measurements of this type utilize simple modifications of the well known megacycle pulse-echo technique. Early measurements were restricted to velocity change with applied hydrostatic pressure. For a cubic crystal, this gives three experimental numbers which are related to five of the six third order elastic constants. Such results are expressed in terms of the pressure derivatives of the three measured second order elastic constants. The original work in this area was done by Lazarus[4] in 1949 and included measurements on Cu, Al, and beta brass. Later, Daniels and Smith[5] reported pressure derivatives of the noble metals Cu, Ag, and Au. Schmunk and Smith[6] made similar measurements on the simple metals Al and Mg. Measurements on the alkali metals Li, Na, and K have also been reported.[7-9] Typically, these measurements utilized hydrostatic pressures in the kilobar region. Such pressures are sufficient to produce readily measurable changes in the transit time of an ultrasonic pulse. A correction for the change in path length with increasing pressure is required.

As stated, hydrostatic pressure measurements on cubic crystals will only give information on three linear combinations of the third order elastic constants. To obtain sufficient information to measure all six third order elastic constants, it is necessary to utilize a deviatoric stress such as uniaxial compression. Here a basic problem arises. In the study of metal single crystals, uniaxial compressions large enough to produce directly measurable changes in the transit time of an ultrasonic pulse will also likely produce changes in the dislocation network always present in the metal crystals. It is well known that dislocations will affect the measured sound velocity. If the applied uniaxial compression changes the existent dislocation network, for example by causing

breakaway from weak pinning points or activation of dislocation sources, a dislocation contribution will be present in the measured sound velocity stress derivative. Hence, we are restricted to very small uniaxial compressions. If measurements can be obtained at several tens of bars, dislocation effects might be avoided. However, stresses of this magnitude will generally produce sound velocity changes of only several parts per million. Uniaxial stress measurements will require an electronic system capable of detecting sound velocity changes at this level.

Several methods have been devised to detect very small sound velocity changes. These have recently been summarized by Alers.[10] In the continuous wave resonance method, the impedance of an ultrasonic transducer-specimen combination is monitored. Rapid variations in the impedance occur as the continuous wave frequency varies through an acoustic resonance associated with standing waves in the specimen. In the phase comparison method, the phase of a megacycle pulse which has transversed the specimen is compared with that of a reference signal. Several variations of this method have been utilized. An important variation, not described by Alers, is the pulse superposition technique of McSkimin,[11,12] in which a series of echoes is superimposed in a phase coherent manner by varying the repetition rate. A second variation of particular interest is the two specimen interferometer first described by Espinola and Waterman.[13] Here a reference pulse is obtained from a second specimen which has been matched to the first. The reference phase depends upon the transit time in the second specimen which can be adjusted by varying the temperature of this specimen. In the sing-around method, two transducers are attached to one specimen, one used as a transmitter and one as a receiver. A particular pulse of the

received signal is used to retrigger the system in such a manner as to create a high stability oscillator whose frequency depends directly on the inverse of the specimen transit time.

The two specimen interferometric technique has been used by Hiki and Granato[14] to measure the complete set of third order elastic constants of the noble metals Cu, Ag, and Au. Their measurements included both hydrostatic and uniaxial stress derivatives. The specimens were prestressed to minimize dislocation effects. Swartz[15] used the same techniques for measurements on beta brass. Salama and Alers[16] repeated uniaxial stress measurements on Cu at several temperatures using the sing-around method. Their room temperature values agree well with Hiki and Granato. They also completed measurements at helium temperatures, the only such measurements which exist at the present time.

Recently, Thurston and Brugger[17] have presented an extremely convenient formulation for obtaining third order elastic constants from sound velocity stress derivatives. The above results for the third order elastic constants of metals have all utilized this formulation. Thurston and Brugger defined a quantity called the natural velocity, $W = 2L_o/t$, where L_o is the path length in the unstressed crystal and t is the round trip transit time. The derivative $\frac{\partial}{\partial P}(\rho_o W^2)_{T,P=0}$ was then evaluated in terms of linear combinations of the third order elastic constants for the various combinations of pure sound modes and applied stress P. Here ρ_o is the density of the unstressed medium. But $(\rho_o W^2)$ will vary with stress simply as t^{-2}. The formulation is convenient because we no longer need to worry about the variation of the path length in the stressed crystal. Also, care was taken to distinguish between adiabatic and isothermal processes. It was pointed out that the third order elastic

constants measured in such experiments are of a mixed nature. Specifically, the quantities measured are

$$C^{ST}_{ijklmn} = \frac{\partial}{\partial \eta_{mn}} \left[\rho_o \frac{\partial^2 U}{\partial \eta_{ij} \partial \eta_{kl}} \right]_S \Bigg]_T \qquad (10)$$

where the isothermal variation refers to the application of the bias stress.

The formulation of Thurston and Brugger along with the recent development of techniques for the measurements of very small sound velocity changes provide a firm basis for the initiation of a program for the measurement of third order elastic constants. In particular, the third order elastic constants of metals would be expected to provide useful new information on the nature of the cohesive properties and interatomic forces of metal crystals. In addition, as has been mentioned above, the third order elastic constants are useful in the calculation of mechanical and thermal properties related to the anharmonic nature of the lattice.

The third order elastic constants of the noble metals[14,16] and beta brass[15] recently obtained confirm the expectation regarding new information on interatomic forces. If it is assumed that the interatomic forces in these crystals are predominantly short range central forces, the following relations would hold among the third order elastic constants:[14] For an FCC lattice with nearest neighbor interactions only,

$$\begin{aligned} C_{111} &= 2C_{112} = 2C_{166} \\ C_{123} &= C_{144} = C_{456} = 0 \ . \end{aligned} \qquad (11)$$

For a BCC lattice with nearest neighbor interactions only,

$$C_{111} = C_{112} = C_{166} = C_{123} = C_{144} = C_{456} \ . \qquad (12)$$

Here the six non-zero third order elastic constants of a cubic crystal are expressed in the contracted (Voight) notation. For a BCC lattice, the next nearest neighbors, the adjacent body-centered atoms, are but 14% more distant than the nearest neighbors. If BCC next nearest neighbor interactions are important, this would result in a contribution to C_{111} only. Results for the noble metals (FCC) correspond closely to the pattern of Eq. (11). The results for beta brass (BCC) correspond closely to Eq. (12) with a significant contribution to C_{111} from the next nearest neighbor interactions. The results for these crystals conform closely to the pattern expected if short range central forces make a predominant contribution to the higher order elastic constants. An important conclusion, then, is that the conduction electrons seem to play a minor role. This might be considered somewhat surprising but can be understood in terms of the existence of overlapping electronic d-shells and the resulting strong exchange forces.

It would be interesting to investigate a material in which the conduction electrons would be expected to make a major contribution to the higher order elastic constants and, hence, to the anharmonic properties of the material. One such material is aluminum. In Al there are no d-electrons; the ion cores are small; and the exchange interactions between ion cores should be negligible. Also, Al has three valence electrons per atom. Hence, the Fermi surface will interact strongly with the Brillouin zone. The conduction electrons should contribute to the shear as well as the compressive elastic constants.

It is the purpose of this thesis to measure the third order elastic constants of single crystal Al. This is done by measuring both hydrostatic pressure and uniaxial stress derivatives of the natural sound

velocities. The results are analyzed within the formalism developed by Thurston and Brugger.[17] The thermal expansion at both high and low temperatures is calculated from the third order elastic constants and compared to the measured values. Finally, an attempt is made to interpret the elastic constants in terms of the cohesive properties of the Al lattice.

II. EXPERIMENTAL PROCEDURE

A. Specimen Preparation

The four aluminum single crystals used in this investigation were of dimensions 15x16x17 mm. They were oriented with faces perpendicular to [110], [1$\bar{1}$0], and [001] directions. These orientations were checked with Laue back reflection photographs and were found to be accurate to better than 1°. The crystals were obtained as oriented from Semi-Elements Inc., Saxonburg, Pennsylvania.

A spectrochemical analysis of the composition of these crystals was obtained from Dr. V. Mossotti of the Materials Research Laboratory, University of Illinois. Order of magnitude estimations of impurity concentrations were determined by emission spectroscopy. The results showed that Cu, Fe, In, Ga, Ca, and Ti were present in concentrations of 10 - 100 parts per million (ppm). Hence, we estimated that the crystals were between 99.95% and 99.99% pure Al.

In order to make sound velocity measurements by the use of a pulse-echo technique, it was necessary to polish the crystals so that opposite faces would be flat and parallel to better than 50 ppm. A convenient method has been developed to obtain such tolerances with moderate effort.[18] The crystals were placed in a cylindrical holder which was relieved in the center and had a 1/8 inch lip around the circumference. The lip surface was machined flat and parallel to better than 100 ppm, and the vertical dimension was set several mils larger than the relevant crystal dimension. The crystal was set in the holder with Quick Mount (Fulton Metallurgical Products) and could be removed after soaking for 24 hours in ethylene dichloride. For rough polishing, 3/0 Emery polishing paper saturated with kerosene was placed on a surface plate. Polishing continued

until the holder and crystal were being cut evenly on both sides. Fine polishing to achieve final tolerances was done with 9.5 micron aluminum oxide powder in a suitable lubricating oil directly on the surface plate. The dimensions were checked on a Mikrokator (C. E. Johanson Co.) which is capable of reading relative values to 10 microinches. A still smoother surface could have been obtained by going to a finer powder, but some surface roughness was desirable to aid in bonding a quartz transducer to the metal surface.

The second order elastic constants of the Al crystals were then measured using a direct pulse-echo technique. Quartz transducers of resonant frequency 10 MHz were attached to the crystal faces with Nonaq stopcock grease (Fisher Scientific Co.). An Arenberg PG-650C pulsed oscillator was used to supply 10 MHz pulses of approximately 3 microsecond duration. Unrectified echoes were received directly by a Tektronix 585A dual time base oscilloscope. The time delay circuit of the oscilloscope was calibrated using a Tektronix 184 crystal time mark generator. The time intervals between a particular cycle of successive echoes could be obtained to better than 10 nsec. A 100 nsec/echo transit time correction was applied to the measurement of longitudinal waves. A measured density of 2.702 $gm.cm^{-3}$ was used in calculating the elastic constants. The results for the second order elastic constants are presented in Table 1 and compared with the values of Schmunk and Smith[6] and Kamm and Alers.[19]

For the particular orientation of our crystals, we were able to obtain eight measurements of four pure mode velocities. The errors presented with our results in Table 1 represent the consistency of these eight measurements as derived from a least squares fit of the data. The

Table 1. The second order elastic constants of Aℓ at 25°C. The errors indicated in column 2 represent the consistency of the measured values. (units of 10^{12} dyn·cm^{-2})

C	This Experiment	Schmunk and Smith[6]	Kamm and Alers[19]
C_{11}	1.0675 ± 0.0005	1.0732	1.0686
C_{12}	0.6041 ± 0.0008	0.6094	0.6075
C_{44}	0.2834 ± 0.0004	0.2832	0.2824
$\frac{1}{2}C_{11} + \frac{1}{2}C_{12} + C_{44}$	1.1192	1.1245	1.1205
$\frac{1}{2}C_{11} - \frac{1}{2}C_{12}$	0.2317	0.2319	0.2305
$\frac{1}{3}C_{11} + \frac{2}{3}C_{12}$	0.7585	0.7640	0.7612

absolute error in the measured elastic constants (C_{11}, $\frac{1}{2}C_{11} + \frac{1}{2}C_{12} + C_{44}$, C_{44}, $\frac{1}{2}C_{11} - \frac{1}{2}C_{12}$ of Table 1), allowing for uncertainties in the transit time measurement, is approximately $\pm$ 0.5%. The measured elastic constants in Table 1 agree within this figure. The fact that the consistency error is much lower than the absolute error is taken as a final indication that the Al specimens were well-oriented single crystals with no important lineage structure.

During the course of the investigation, it was decided to neutron irradiate two of the Al crystals. The irradiation took place in the CP-5 reactor at the Argonne National Laboratory. The integrated exposure was approximately 5×10^{18} neutrons per cm^2 with energy greater than 100 keV. The temperature of the crystals was neither monitored nor controlled during the irradiation.

B. Ultrasonic Interferometer

For measurements of the natural sound velocity stress derivatives, we have used the two specimen ultrasonic interferometric technique. The interferometer is illustrated in Fig. 1. The oscillator and receiver were contained in a single unit, the Matec attenuation comparator. The Tektronix 585A oscilloscope was used to observe the rectified signal output of the Matec unit. This allowed observation of an expanded region of the echo pattern at any desired transit time. The method is basically the same as that described by Hiki and Granato[14] and by Swartz.[15] We give here a brief description together with a closer analysis of some aspects of the measurement found to be particularly important in this experiment.

The generation of an ultrasonic interference pattern can be described qualitatively as follows: Quartz transducers were attached to

Fig. 1. The ultrasonic interferometer. The oscillator and receiver are contained in a single unit, the Matec attenuation comparator.

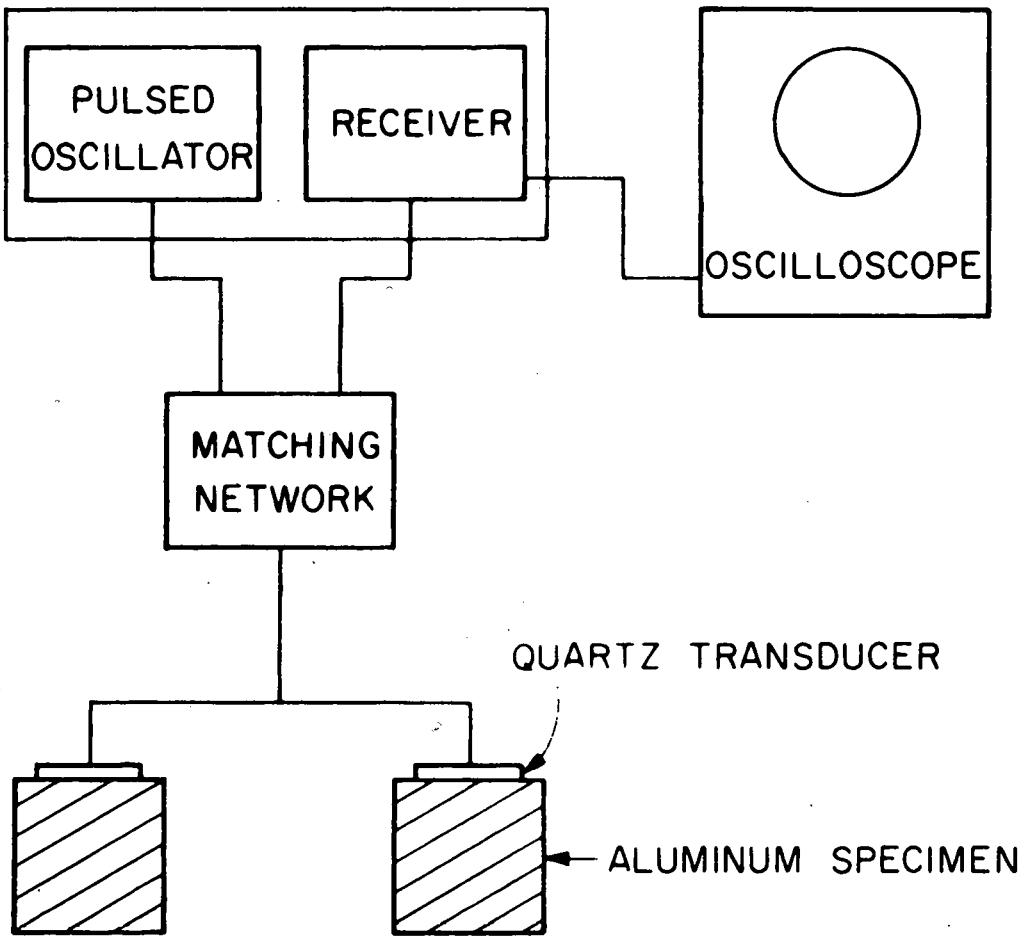
PULSED
OSCILLATOR
RECEIVER
OSCILLOSCOPE
MATCHING
NETWORK
QUARTZ TRANSDUCER
ALUMINUM SPECIMEN

both specimens, and the same pulse was applied to each. The two specimens were polished together and, hence, the path lengths were well matched. If the temperature and pressure were the same for the two specimens, the wave velocities would be identical. Hence, the two echo patterns obtained would also be identical. When viewed in parallel, they would simply add. Now, if a temperature difference of a few degrees centigrade was set between the specimens, the resulting wave velocity difference would be sufficient to cause a readily observable interference pattern.

Temperature control was an important aspect of the experiment. It was necessary to be able to detect small changes in the temperature difference between the two specimens and to control the rate at which this temperature difference changed. To measure small changes in the temperature difference, we used the following technique: Chromel - Advance (5 mil diameter wire) thermocouples were attached to the specimens. The sensitivity of these thermocouples was nearly 60 microvolts per °C. The emf representing the temperature difference was measured by a Minneapolis - Honeywell 2768 microvolt potentiometer. The unbalance potential of the potentiometer was then fed into a Leeds and Northrup dc amplifier and AZAR strip chart recorder. The amplifier - recorder combination was set for a full scale deflection of 10 microvolts. With this arrangement, temperature changes of approximately two millidegrees could be detected. The rate of change of the temperature difference was controlled as follows: The stressed specimen was effectively at room temperature. The second specimen was placed in a furnace which, in turn, was immersed in an ice bath. By adjusting the current in the furnace coils, the temperature and temperature rate of change of this specimen could be controlled as desired between approximately 0°C and 20°C.

The application of hydrostatic pressure and uniaxial compression was accomplished as follows: The hydrostatic pressure was obtained simply by using nitrogen tank gas. The pressure was measured by a Heise bourdon gage. The uniaxial compression was applied by a Tinius Olsen universal testing machine operated in the constant load mode. The machine calibration was checked with a Morehouse proving ring and was found to be accurate to better than 0.5% at full load. During loading the crystal being stressed was placed between indium shims, and the stress was applied through a ball joint to insure uniform uniaxial compression. For each type of loading, the stress range was approximately 0-50 $kg \cdot cm^{-2}$.

In the formulation of Thurston and Brugger,[17] the third order elastic constants are expressed in terms of $\frac{\partial}{\partial P}(\rho_o W^2)_{T,P=0}$ where W is the natural velocity defined previously. This can be written as

$$\frac{\partial}{\partial P}(\rho_o W^2)_{T,P=0} = 2w \left(\frac{1}{W_o} \frac{\partial W}{\partial P} \right)_{T,P=0} . \tag{13}$$

Here w is the second order elastic constant $(\rho_o W^2)_{P=0}$. If we consider W to be a simple thermodynamic function of two variables, W = W(P,T), then

$$\frac{1}{W_o} \left.\frac{\partial W}{\partial P}\right|_T = - \frac{1}{W_o} \left.\frac{\partial W}{\partial T}\right|_P \left.\frac{\partial T}{\partial P}\right|_W . \tag{14}$$

Equation (14) indicates the procedure we followed in measuring the natural velocity stress derivatives using the two specimen interferometer. We first measured $\frac{1}{W_o} \left.\frac{\partial W}{\partial T}\right|_P$ for a particular sound mode. This could be considered as a calibration of the interferometer for this mode. We then measured $\partial T/\partial P|_W$ for the various stress derivatives of the mode.

Direct measurement of the temperature derivative $\frac{1}{W_o}\frac{\partial W}{\partial T}\Big|_P$ was carried out according to the method of Espinola and Waterman.[13] They relate the velocity difference of two superimposed waves to the observed interference condition. If the velocity difference is caused entirely by a temperature difference between the two specimens, we can write

$$\frac{1}{W_o}\frac{\partial W}{\partial T}\Big|_P = \frac{2j-1}{2f\ t_o}\ \frac{\partial}{\partial T}\ \left(\frac{1}{n}\right) \quad . \tag{15}$$

Here f is the frequency; t_o is the round trip transit time; j is the node index; and n is the echo index. We measured the temperature difference ΔT between the two specimens for which the j^{th} node is at the n^{th} echo. It was observed that 1/n is a linear function of ΔT. This gave the expected linear dependence of wave velocity on temperature. The temperature range for each measurement was less than 10°C.

These results can be expressed in terms of the temperature dependence of the second order elastic constant, $c = \rho v^2$. Here ρ is the density, and v is the actual sound velocity. Hence, the temperature dependence of c is given by

$$\frac{\partial c}{\partial T}\Big|_P = c\left(\frac{2}{W_o}\ \frac{\partial W}{\partial T}\Big|_P - \alpha\right) \quad . \tag{16}$$

Here α is the coefficient of linear thermal expansion (0.234×10^{-4} °C^{-1} for Al at 25°C).[20]

The results for $\frac{1}{W_o}\frac{\partial W}{\partial T}\Big|_P$ for the four sound modes which could be propagated in our specimens are presented in Table 2. The results for $\partial c/\partial T|_P$ are presented in Table 3 and are compared to the results of Long and Smith[21] and Kamm and Alers.[19] Kamm and Alers present their results

in tabular form, and we have calculated the derivative from their high temperature values.

Certain inconsistencies were present in our data for the temperature derivatives. It was found that these could be explained by considering the existence of an initial phase difference between the two waves. The analysis of Espinola and Waterman[13] has been extended to account for such effects. This work is presented in Appendix A. Also, difficulties were encountered in measurements on the ⟨110⟩ longitudinal mode wave velocity. In particular, repeated measurements of the temperature derivative of this mode showed excessively high scatter (approximately 15% of the final value). It was decided to use only the results for the temperature derivatives of the other three modes. A value for the ⟨110⟩ longitudinal mode was calculated from these three modes. This calculated value fell well within the range of the measured values. We have no definite explanation of the difficulties with the ⟨110⟩ longitudinal mode. Results for the other three modes were satisfactory. The error presented with our results in Table 3 represents the range of values observed for these three measured temperature derivatives.

We then measured $\partial T/\partial P|_W$. To do this we picked a convenient interference pattern as described above by setting the appropriate temperature difference ΔT between the two specimens. We defined the interference condition exactly by noting the relative echo amplitudes near a particular node. If the stress on one specimen was changed by δP, the interference pattern changed. That is, the relative echo heights near the observed node changed. An appropriate change in the temperature difference, $\delta(\Delta T)$, would then return the system to the initial interference pattern.

Table 2. The temperature derivatives of the natural velocities of $A\ell$. These can be considered as a calibration of the interferometer for the various modes. (units of 10^{-4} $°C^{-1}$)

Sound Mode	$\frac{1}{W}\frac{\partial W}{\partial T}\Big\|_P$
C_{11}	- 1.53
$\frac{1}{2}C_{11} + \frac{1}{2}C_{12} + C_{44}$	- 1.47
$\frac{1}{2}C_{11} - \frac{1}{2}C_{12}$	- 2.95
C_{44}	- 2.44

Table 3. The temperature derivatives of the second order elastic constants of Aℓ. The errors indicated in column 2 represent the range of the measured values as described in the text. (units of 10^8 dyn.cm^{-2}.°C^{-1})

$$\frac{\partial c}{\partial T}\Big|_P$$

c	This Experiment	Long and Smith[21]	Kamm and Alers[19]
C_{11}	- 3.51 ± 0.10	- 3.44	- 3.75
C_{12}	- 0.69	- 0.98	- 0.55
C_{44}	- 1.45 ± 0.05	- 1.43	- 1.43
$\frac{1}{2}C_{11} + \frac{1}{2}C_{12} + C_{44}$	- 3.55	- 3.64	- 3.58
$\frac{1}{2}C_{11} - \frac{1}{2}C_{12}$	- 1.42 ± 0.05	- 1.23	- 1.60
$\frac{1}{3}C_{11} + \frac{2}{3}C_{12}$	- 1.62	- 1.8	- 1.65

By making successive changes of this type about the initial interference pattern as a null condition, we determined $\delta(\Delta T)/\delta P = \partial T/\partial P|_W$.

The sensitivity of the two specimen technique depends upon the smallest wave velocity change which will produce an observable change in an interference pattern. This, in turn, depends upon the structure of the interference pattern and the position in time at which measurements are being obtained. In general, the sensitivity is higher at longer transit times. We have observed that changes of the order $\delta W/W = 2 \times 10^{-6}$ can be detected for waves which have spent 100-150 microseconds in the crystal.

This completes the description of the ultrasonic interferometer. Extensive measurements by Swartz[22] on NaCl have demonstrated that the two specimen interferometer gives reliable results compatible with one specimen techniques. The two specimen technique has the distinct advantage that small temperature drifts of the stressed specimen will not obscure the sound velocity change with pressure. The two specimen technique depends explicitly on the temperature difference between the two specimens. It is irrelevant which specimen actually changes temperature.

III. EVALUATION OF THIRD ORDER ELASTIC CONSTANTS

A sound wave can be described by a propagation direction $\underline{N}$, a displacement (or polarization) direction $\underline{U}$, and an effective second order elastic constant, $w = (\rho_o W^2)_{P=0}$. For an unstressed configuration, w can be expressed in terms of a linear combination of the second order elastic constants defined by Eq. (9). For the particular orientation of our crystals, we were able to propagate five different pure mode sound waves, two longitudinal and three transverse. We measured the hydrostatic pressure derivatives of the natural velocities of these five waves. We also measured nine uniaxial stress derivatives of the five natural velocities. These 14 experiments are characterized in Table 4.

Thurston and Brugger[17] have given explicit relations between the measured quantities $\frac{\partial}{\partial P}(\rho_o W^2)_{T,P=0}$ and the second and third order elastic constants for the 14 experiments described in Table 4. These relations are presented in Table 5. In Table 5, the superscript T indicates an isothermal elastic constant.

We first measured the hydrostatic pressure derivatives of the five natural sound velocities, expts. 10-14 of Table 5. Measurements were taken on two sets of crystals, and the results for each mode were averaged. The natural sound velocity change for a typical hydrostatic experiment is illustrated in Fig. 2. The results were expressed in terms of three linear combinations of five of the six third order elastic constants, $(C_{111} + 2C_{112})$, $(\tfrac{1}{2}C_{111} - \tfrac{1}{2}C_{123})$, $(C_{144} + 2C_{166})$. These three numbers were determined by a least squares fit of the five measurements. The results are presented in the first row of Table 6. The error indicated with these results represents the consistency of the five measurements.

Table 4. Characterization of sound velocity stress experiments.

Expt. No.	Propagation Direction $\underline{N}$	Displacement Direction $\underline{U}$	Stress Direction $\underline{M}$	$w = (\rho_o W^2)_{P=0}$
1	[110]	[110]	[001]	$\frac{1}{2}C_{11} + \frac{1}{2}C_{12} + C_{44}$
2	[1$\bar{1}$0]	[1$\bar{1}$0]	[001]	$\frac{1}{2}C_{11} - \frac{1}{2}C_{12}$
3	[110]	[001]	[001]	C_{44}
4	[001]	[001]	[110]	C_{11}
5	[001]	[110]	[110]	C_{44}
6	[001]	[1$\bar{1}$0]	[110]	C_{44}
7	[1$\bar{1}$0]	[110]	[1$\bar{1}$0]	$\frac{1}{2}C_{11} + \frac{1}{2}C_{12} + C_{44}$

Table 4. (continued)

Expt. No.	N	U	M	w
8	[110]	$[1\bar{1}0]$	$[1\bar{1}0]$	$\frac{1}{2}C_{11} - \frac{1}{2}C_{12}$
9	[110]	[001]	$[1\bar{1}0]$	C_{44}
10	[001]	[001]	Hyd.	C_{11}
11	[001]	any $\perp$ N	Hyd.	C_{44}
12	[110]	[110]	Hyd.	$\frac{1}{2}C_{11} + \frac{1}{2}C_{12} + C_{44}$
13	[110]	$[1\bar{1}0]$	Hyd.	$\frac{1}{2}C_{11} - \frac{1}{2}C_{12}$
14	[110]	[001]	Hyd.	C_{44}

Table 5. Natural sound velocity stress derivatives as a function of second and third order elastic constants.

Expt. No.	$\frac{\partial}{\partial P}(\rho_o W^2)_{T,P=0}$
1	$2wa + \frac{1}{2}aC_{111} + \frac{1}{2}(3a-b)\,C_{112} - \frac{1}{2}bC_{123} - bC_{144} + 2a\,C_{166}$
2	$2wa + \frac{1}{2}aC_{111} - \frac{1}{2}(a+b)\,C_{112} + \frac{1}{2}bC_{123}$
3	$-2wb + aC_{144} + (a-b)\,C_{166}$
4	$2wa + aC_{111} + (a-b)\,C_{112}$
5	$w(a-b-2c) + \frac{1}{2}(a-b)\,C_{144} + \frac{1}{2}(3a-b)\,C_{166} - 2c\,C_{456}$
6	$w(a-b+2c) + \frac{1}{2}(a-b)\,C_{144} + \frac{1}{2}(3a-b)\,C_{166} + 2c\,C_{456}$
7	$w(a-b+2c) + \frac{1}{4}(a-b)\,C_{111} + \frac{1}{4}(5a-3b)\,C_{112} + \frac{1}{2}aC_{123} + aC_{144} + (a-b+4c)\,C_{166}$
8	$w(a-b-2c) + \frac{1}{4}(a-b)\,C_{111} + \frac{1}{4}(a+b)\,C_{112} - \frac{1}{2}aC_{123}$
9	$2wa + \frac{1}{2}(a-b)\,C_{144} + \frac{1}{2}(3a-b)\,C_{166} + 2c\,C_{456}$

Table 5. (continued)

Expt. No.	$\frac{\partial}{\partial P}(\rho_o W^2)_{T,P=0}$
10	$-1-2w(2a-b) + (2a-b)\,[C_{111} + 2C_{112}]$
11	$-1-2w(2a-b) + (2a-b)\,[C_{144} + 2C_{166}]$
12	$-1-2w(2a-b) + (2a-b)\,[\frac{1}{2}C_{111} + 2C_{112} + \frac{1}{2}C_{123} + C_{144} + 2C_{166}]$
13	$-1-2w(2a-b) + (2a-b)\,[\frac{1}{2}C_{111} - \frac{1}{2}C_{123}]$
14	$-1-2w(2a-b) + (2a-b)\,[C_{144} + 2C_{166}]$

$$a = \frac{C_{12}^{T}}{3B^{T}(C_{11}^{T}-C_{12}^{T})}, \quad \gamma = \frac{C_{11}^{T}+C_{12}^{T}}{3B^{T}(C_{11}^{T}-C_{12}^{T})}, \quad c = \frac{1}{4C_{44}}$$

$$3B^{T} = C_{11}^{T} + 2C_{12}^{T}$$

$$C_{11}^{T} = 1.0339 \times 10^{12}\ \text{dyn.cm}^{-2}, \quad C_{12}^{T} = 0.5104 \times 10^{12}\ \text{dyn.cm}^{-2}$$

Fig. 2. Natural velocity change vs. hydrostatic pressure for a C_{44} mode (Expt. 14 of Tables 4 and 5). The separation between the curves for increasing and decreasing pressure is due to a thermal lag between the surface and bulk of the specimen of approximately 0.1°C. To reduce any effect on the measured slope, the results for increasing and decreasing pressure were averaged.

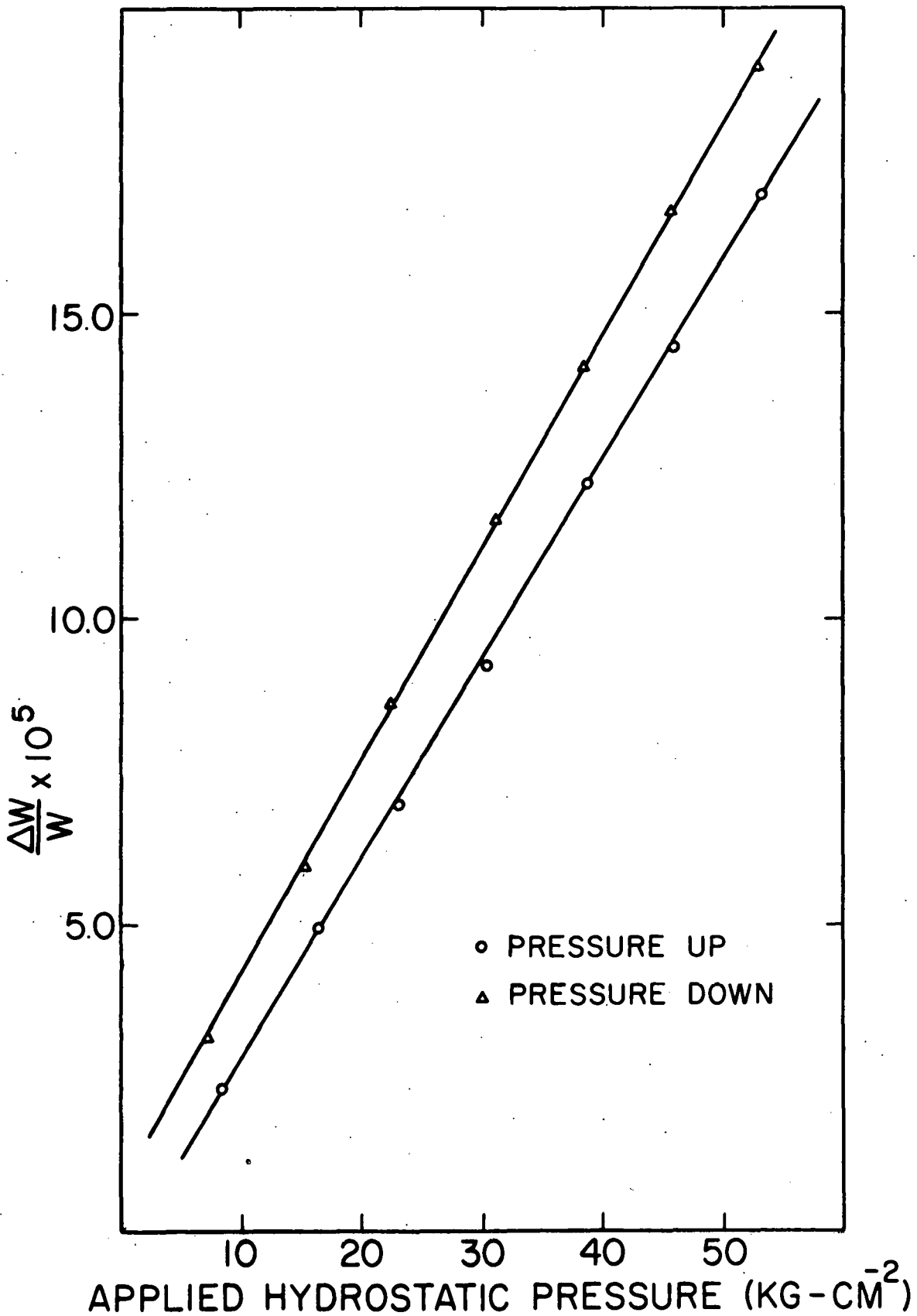
15.0
10.0
5.0
$\frac{\Delta W}{W} \times 10^5$
PRESSURE UP
PRESSURE DOWN
10
20
30
40
50
APPLIED HYDROSTATIC PRESSURE (KG-CM^{-2})

Initial uniaxial stress measurements were made on the two sets of crystals. The stress range was approximately 0-40 $kg \cdot cm^{-2}$. Even in this small stress region, we expected that dislocation motion might occur. Hiki and Granato[14] found that an initial prestress was effective in eliminating dislocation effects in measurements on noble metals. That method was also attempted here. The sound wave attenuation was monitored during the prestress, and no significant changes were detected. However, it became apparent that dislocation effects were present in the initial uniaxial data.

The problem of determining whether or not dislocation effects exist in a particular uniaxial experiment or series of experiments is quite involved. Initially, it was hoped that for any particular experiment a dislocation contribution would be a non-linear function of applied stress, easily distinguishable from the patently linear lattice effect. Hiki and Granato[14] observed a highly non-linear velocity change at stresses above their prestress level. However, Salama and Alers[16] discounted this simple notion. Their measurements on hardened Cu crystals showed that the uniaxial data could be linear, reproducible, show no hysteresis, and give no attenuation change with applied stress and could still contain a dislocation contribution. However, they suggested that a suitable criterion for the absence of dislocation effects in a series of uniaxial measurements was that hydrostatic pressure derivatives calculated from the uniaxial data be in agreement with the directly measured values.

We have adopted that criterion here. This is reflected in the method of data reduction. The nine uniaxial stress experiments give information on eight linear combinations of the six third order elastic constants. The uniaxial data could be used alone to obtain a set of

third order elastic constants. The three linear combinations related to the hydrostatic pressure derivatives could then be calculated from this set. If substantial agreement could be obtained between the measured and calculated values of these three linear combinations, then it would be proper to combine all the data and obtain a self-consistent set of third order elastic constants and hydrostatic pressure derivatives.

The dominant characteristic of the initial uniaxial data was that expts. 1, 2, 3, 4, 7, and 8 gave a linear dependence of the change in natural velocity with stress while expts. 5, 6, and 9 did not. A typical linear natural velocity change is illustrated in Fig. 3. In the non-linear experiments, a hysteresis effect was observed which was qualitatively reproducible. A typical non-linear natural velocity change including hysteresis is illustrated in Fig. 4.

The six linear experiments were related to five of the six third order elastic constants. These were the same five constants which determined the hydrostatic pressure derivatives. The initial uniaxial data from the six linear experiments was used to determine these five elastic constants by a least squares analysis. The set of third order constants so determined was totally inconsistent with the measured hydrostatic pressure derivatives. For example, after a particular set of measurements, we obtained $(C_{111} + 2C_{112}) = -8.20 \times 10^{12}$ dyn·cm^{-2} compared to the measured value of -17.10 in the same units. Dislocation effects were obviously present in the non-linear experiments. It was concluded that dislocation effects must also have been present in several of the linear experiments.

One set of Al crystals was then neutron irradiated as described in Sec. IIA. The uniaxial stress measurements were then repeated.

Fig. 3. Natural velocity change vs. applied uniaxial stress for a C_{44} mode (Expt. 3 of Tables 4 and 5). The experiment was begun with a 4 $kg \cdot cm^{-2}$ setting stress applied to the specimen.

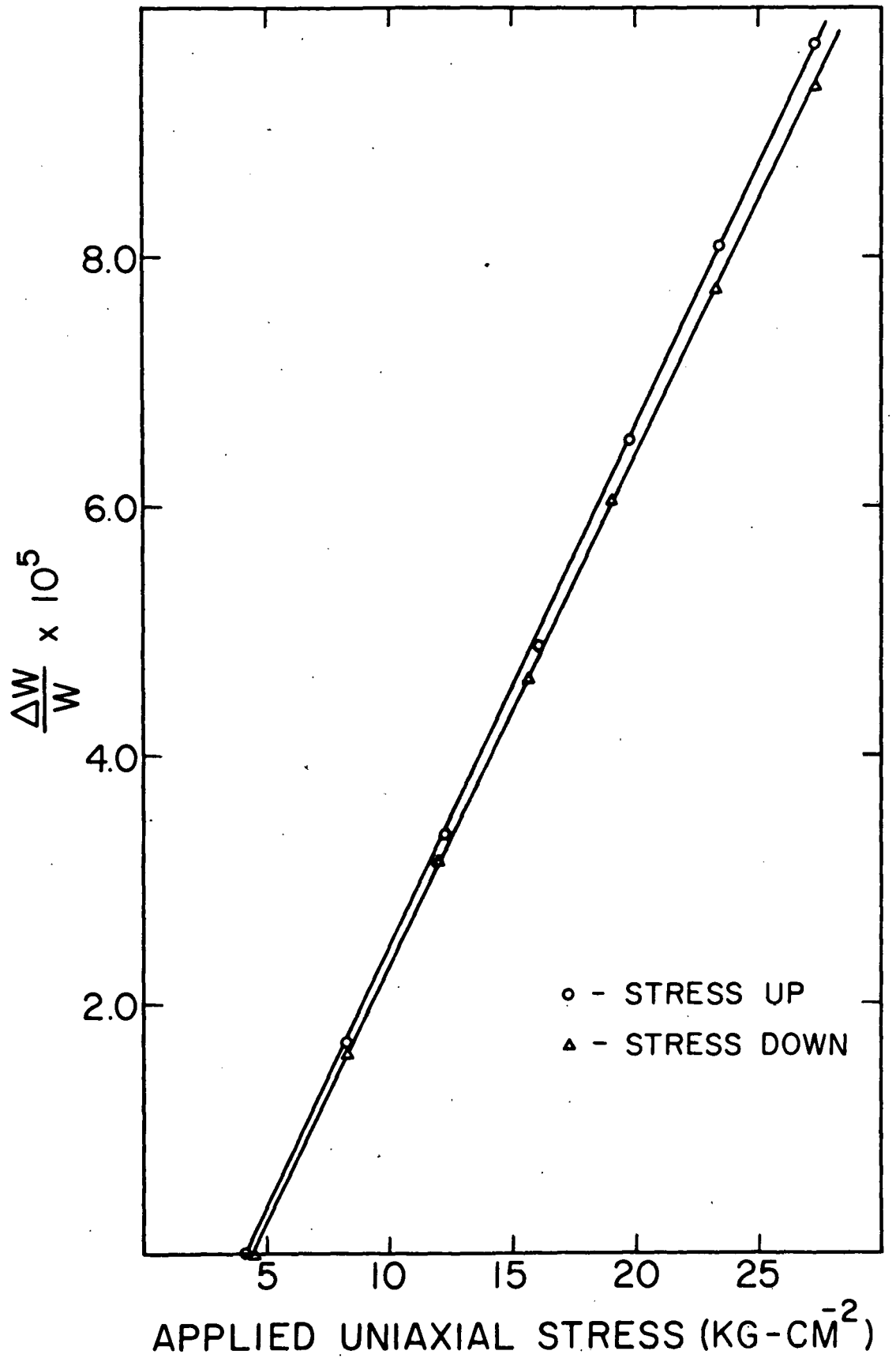
8.0
6.0
4.0
2.0
$\frac{\Delta W}{W} \times 10^5$
5
10
15
20
25
APPLIED UNIAXIAL STRESS (KG-CM^{-2})
o - STRESS UP
Δ - STRESS DOWN

Fig. 4. Natural velocity change vs. applied uniaxial stress for a typical non-linear mode (Expt. 9 of Tables 4 and 5). The observed hysteresis is attributed to a dislocation effect.

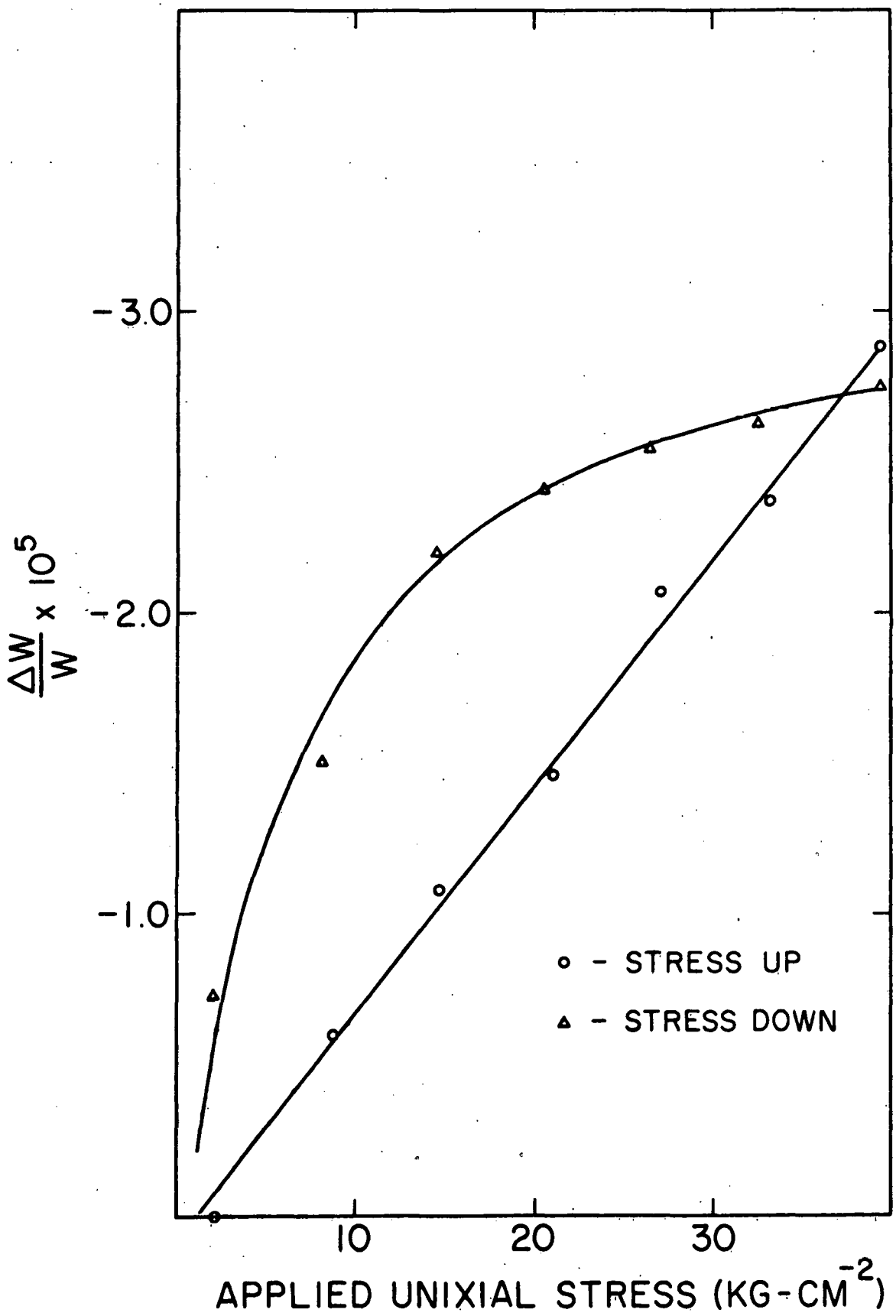
-3.0
-2.0
-1.0
$\frac{\Delta W}{W} \times 10^5$
10
20
30
APPLIED UNIXIAL STRESS (KG-CM^{-2})
o - STRESS UP
Δ - STRESS DOWN

Results for expts. 2, 3, 5, 6, and 9 were essentially unchanged. The hysteresis effects observed in the latter three of these experiments were still present. The result for expts. 1, 4, 7, 8 changed substantially. The measured natural velocity changes with stress all became algebraically larger. This is the direction of change one would expect if dislocation effects had been eliminated. The six linear experiments were again analyzed to obtain a least squares fit for five of the six third order elastic constants. The three linear combinations of the third order elastic constants related to the hydrostatic pressure derivatives calculated from these results agreed almost exactly with the measured values. These combinations are presented in the second row of Table 6. The error presented represents the consistency of the six uniaxial measurements.

Results of expts. 5, 6, and 9 on the irradiated crystals still showed hysteresis effects similar to that illustrated in Fig. 4. It is very likely that the observed hysteresis effects are associated with microscopic plastic flow. Some dislocation motion must still be occurring in the irradiated crystals. However, because of the excellent agreement observed in Table 6 between uniaxial and hydrostatic measurements, we conclude that dislocation effects have been effectively eliminated from the six linear uniaxial experiments.

We then combined the acceptable uniaxial and hydrostatic data to obtain a self-consistent set of third order elastic constants and hydrostatic pressure derivatives. The data used in this calculation are summarized in columns 2-4 of Table 7. Results for the natural velocity stress derivatives (Eq. (14)) are presented in the fifth column and for $\frac{\partial}{\partial P}(\rho_o W^2)_{T,P=0}$ (Eq. (13)) in the sixth column of this table. The errors

Table 6. The third order elastic constants related to sound velocity hydrostatic pressure derivatives. The errors indicated represent the consistency of each set of measurements. (units of 10^{12} dyn. cm^{-2})

Measurement	$C_{111} + 2C_{112}$	$\frac{1}{2}C_{111} - \frac{1}{2}C_{123}$	$C_{144} + 2C_{166}$
Hydrostatic	-17.10 ± 0.05	-5.60 ± 0.07	-6.99 ± 0.04
Uniaxial	-17.11 ± 0.04	-5.57 ± 0.02	-7.06 ± 0.01

Table 7. Experimental data and results for natural velocity stress derivatives. The errors indicated in column 4 represent the range of the measured values.

Expt. No.	w ($dyn.cm^{-2}$)	$\frac{1}{W}\frac{\partial W}{\partial T}\Big\|_P$ ($°C^{-1}$)	$\frac{\partial T}{\partial P}\Big\|_W$ ($°C.dyn^{-1}.cm^2$)	$\frac{1}{W}\frac{\partial W}{\partial P}\Big\|_T$ ($dyn^{-1}.cm^2$)	$\frac{\partial}{\partial P}(\rho_o W^2)_{T,P=0}$ (dimensionless)
1	1.1192×10^{12}	-1.47×10^{-4}	$-1.74 \pm 0.10 \times 10^{-8}$	$-2.56 \pm 0.14 \times 10^{-12}$	-5.73 ± 0.32
2	0.2317	- 2.95	0.66 ± 0.04	1.95 ± 0.13	0.90 ± 0.06
3	0.2834	- 2.44	1.78 ± 0.07	4.34 ± 0.16	2.46 ± 0.09
4	1.0675	- 1.53	-0.51 ± 0.05	-0.78 ± 0.08	-1.67 ± 0.16
7	1.1192	- 1.47	-1.04 ± 0.07	-1.53 ± 0.10	-3.42 ± 0.22
8	0.2317	- 2.95	0.23 ± 0.02	0.68 ± 0.04	0.32 ± 0.02
10	1.0675	- 1.53	1.80 ± 0.10	2.75 ± 0.15	5.87 ± 0.32
11,14	0.2834	- 2.44	1.40 ± 0.02	3.42 ± 0.05	1.94 ± 0.03
12	1.1192	- 1.47	1.98 ± 0.02	2.91 ± 0.02	6.51 ± 0.05
13	0.2317	- 2.95	1.01 ± 0.05	2.98 ± 0.15	1.38 ± 0.07

presented with the measured $\partial T/\partial P|_W$ represent the range of several measurements for each mode (on the irradiated crystals only for uniaxial measurements). These numbers are simply scaled to obtain the error presented in the fifth and sixth columns. From the relations of Thurston and Brugger[17] (Table 5) and the measured quantities $\frac{\partial}{\partial P}(\rho_o W^2)_{T,P=0}$, we obtained the five third order elastic constants related to the hydrostatic and linear uniaxial data by a least squares analysis. The final set of third order elastic constants is presented in Table 8. The errors indicated in Table 8 represent the range of measured stress derivatives. These were obtained by substituting various combinations of the maximum and minimum pressure derivatives in the least squares computer program and noting the range of third order elastic constants so calculated.

Although expts. 5, 6, and 9 were grossly non-linear, certain restrictions on the stress derivative could be deduced. It was clear that the derivative was small in each case. Assuming that the constants C_{144} and C_{166} were well known, a fair estimate of C_{456} could be obtained. This value of C_{456} is presented in Table 8.

The final, self-consistent set of third order elastic constants was used to calculate the hydrostatic pressure derivatives of the second order elastic constants, $c = \rho v^2$. From the definitions of c and W, we determine that

$$\left.\frac{\partial c}{\partial P}\right|_{T,P=0} = \frac{c}{3B^T} + \frac{\partial}{\partial P}(\rho_o W^2)_{T,P=0} . \qquad (17)$$

Here B^T is the isothermal bulk modulus. The second term of Eq. (17) was calculated from the relations in Table 5 (Expts. 10-14) and the measured elastic constants. The results are presented in Table 9 and compared to

Table 8. The third order elastic constants of Aℓ at 25°C. The errors represent the range of measured stress derivatives as discussed in the text. (units of 10^{12} dyn.cm^{-2})

$$C_{111} = -10.76 \pm 0.30$$

$$C_{112} = -3.15 \pm 0.10$$

$$C_{123} = +0.36 \pm 0.15$$

$$C_{144} = -0.23 \pm 0.05$$

$$C_{166} = -3.40 \pm 0.10$$

$$C_{456} = -0.30 \pm 0.30$$

Table 9. The hydrostatic pressure derivatives of the second order elastic constants, $c = \rho v^2$, of Al. The error presented with the results of the experiment is consistent with the error associated with the final set of third order elastic constants.

	$\frac{\partial c}{\partial P}\Big\|_T$	
c	This Experiment	Schmunk and Smith[6]
C_{11}	6.35 ± 0.23	7.35
C_{12}	3.45 ± 0.16	4.11
C_{44}	2.10 ± 0.12	2.31
$\frac{1}{2}C_{11} + \frac{1}{2}C_{12} + C_{44}$	7.00 ± 0.31	8.04
$\frac{1}{2}C_{11} - \frac{1}{2}C_{12}$	1.45 ± 0.10	1.62
$\frac{1}{3}C_{11} + \frac{2}{3}C_{12}$	4.42 ± 0.18	5.19

the results of Schmunk and Smith.[6] The error presented is consistent with the error associated with the final set of third order constants. Our values for the pressure derivatives of the shear constants (C_{44}, $\frac{1}{2}C_{11}-\frac{1}{2}C_{12}$) are in fair agreement with those of Schmunk and Smith. For the longitudinal constants (C_{11}, $\frac{1}{2}C_{11}+\frac{1}{2}C_{12}+C_{44}$), our results are significantly smaller. We have no definite explanation for this. It is interesting to note, however, that a similar comparison can be made regarding noble metals between work at this laboratory (Hiki and Granato[14]) and at Case-Western Reserve (Daniels and Smith[5]). The principal difference between the two experimental techniques is the pressure range, the Case group working at pressures up to 10 kbars. This might adversely affect the specimen-transducer bond. In the following section we investigate this comparison further by using the pressure derivative results to calculate the lattice thermal expansion.

IV. THERMAL EXPANSION AND THE GRÜNEISEN PARAMETER

Within the anisotropic continuum model, the thermal expansion can be calculated from the third order elastic constants. For a cubic crystal, the thermal expansion is isotropic and can be expressed in terms of the pressure derivatives of the three second order elastic constants. Hence, it depends directly upon the three linear combinations of the third order elastic constants previously discussed (Table 6). Comparison of a measured and calculated thermal expansion should provide some information on the magnitude of these three third order constants. Such a program has been discussed elsewhere,[23] but a short account will be given here for completeness. A further discussion will also be given on comparisons at low temperatures.

To calculate the thermal expansion, we used the quasiharmonic approximation. This means that all thermodynamic and elastic properties of a crystal are assumed to be determined by the harmonic lattice frequency distribution and its dependence on volume or, more generally, on strain. This dependence is usually specified by defining the scalar mode Grüneisen parameters,

$$\gamma_i = -\frac{V}{\nu_i}\frac{d\nu_i}{dV} \quad . \tag{18}$$

Here V is the volume of the material, and ν_i is the frequency of the i^{th} normal mode. In the quasiharmonic approximation, ν_i depends only on the state of deformation and is not an explicit function of temperature.[24] Under this assumption, the thermodynamic Grüneisen parameter can be defined as a weighted mean of the individual mode parameters, namely,

$$\gamma = \sum_{i=1}^{3N} C_i \gamma_i \Big/ \sum_{i=1}^{3N} C_i \quad . \tag{19}$$

Here C_i is the specific heat of the i^{th} normal mode. γ is then directly related to the thermal expansion as[25]

$$\gamma = \beta V B_T / C_V = \beta V B_S / C_P \quad . \tag{20}$$

Here V is the molar volume; B_T and B_S are, respectively, the isothermal and adiabatic bulk moduli; C_V and C_P are, respectively, the specific heats at constant volume and constant pressure; and β is the volume thermal expansion. We see that the calculation of the thermal expansion basically reduces to the calculation of the various γ_i and their weighted mean γ. It is convenient to compare measured and calculated values of the thermal expansion through the respective Grüneisen parameters.

In the anisotropic continuum model, Eq. (18) becomes

$$\gamma_i = -\frac{1}{6} + \frac{1}{2} \frac{B_T}{c_i} \left. \frac{\partial c_i}{\partial P} \right|_T \tag{21}$$

Here B_T is the isothermal bulk modulus, and c_i is the effective second order elastic constant of the i^{th} mode. In the quasiharmonic model, the mode parameters are not explicitly temperature dependent. However, the thermodynamic parameter does depend on temperature through the weighting factors (specific heats C_i). Expressions for the high temperature and low temperature limits of the thermodynamic Grüneisen parameter can be obtained from Eq. (19). At high temperatures, $C_i = k$ (the Boltzmann constant) for each of the 3N modes, and

$$\gamma_H = \frac{1}{3N} \sum_{i=1}^{3N} \gamma_i \quad . \tag{22}$$

At low temperatures, by assuming the continuum model, it can be shown that[26]

$$\gamma_L = \sum_{i=1}^{3N} \frac{\gamma_i}{v_i^3} \Bigg/ \sum_{i=1}^{3N} \frac{1}{v_i^3} \quad . \tag{23}$$

Here v_i is the wave velocity of the i^{th} mode. The Grüneisen parameter at intermediate temperatures is usually calculated by taking account of the variation of the specific heat with temperature and the assumed frequency distribution.

Recently Brugger[27] has discussed the tensorial mode Grüneisen parameters

$$\gamma_i^{\alpha\beta} = - \left[\frac{1}{\nu_i} \left(\frac{\partial \nu_i}{\partial \eta_{\alpha\beta}} \right)_T \right]_{\eta=0} \tag{24}$$

which are based upon the general Lagrangian strain dependence of the normal mode frequencies. This parameter is not intrinsically quasiharmonic as an explicit temperature dependence is allowed. However, this dependence is not utilized, and the following calculation can be considered quasiharmonic. Adapting the anisotropic continuum model and appropriate boundary conditions, the $\gamma_i^{\alpha\beta}$ can be written as

$$\gamma_i^{\alpha\beta} = - \frac{1}{2w_i} \left[\frac{\partial \left(\rho_o W_i^2 \right)}{\partial \eta_{\alpha\beta}} \right]_{T,\ \eta=0} \quad . \tag{25}$$

Here W_i is the natural velocity of the i^{th} mode, and $w_i = (\rho_o W_i^2)_{\eta=0}$. By solving the wave equation of small amplitude waves in a homogeneously deformed medium, Thurston and Brugger[17] derived the expression

$$\rho_o W_i^2 U_u = \left[\delta_{uv} \bar{t}_{mn} + \left(\delta_{vw} + 2\bar{\eta}_{vw} \right) \bar{C}^S_{munw} \right] N_m N_n U_v \quad . \tag{26}$$

Here $\underline{N}$ and $\underline{U}$ are the propagation and polarization vectors of the i^{th} normal mode, and t is the thermodynamic tension ($t_{mn} = \rho_o (\partial U/\partial \eta_{mn})_S = \rho_o (\partial F/\partial \eta_{mn})_T$ where U and F are the internal and free energies per unit mass of the material). The bar over a symbol indicates that the quantity is to be evaluated in the homogeneously deformed state. By differentiating Eq. (26) with respect to $\eta_{\alpha\beta}$ and evaluating at $\eta=0$, one obtains an expression for the tensorial mode Grüneisen parameter

$$\gamma_i^{\alpha\beta} = - \frac{1}{2w_i} \left[2w_i U_\alpha U_\beta + \left(C^T_{\alpha\beta mn} + C^{ST}_{\alpha\beta munv} U_u U_v \right) N_m N_n \right] \tag{27}$$

with

$$w_i = C^S_{mumv} N_m N_n U_n U_v \quad . \tag{28}$$

Summation over repeated indices is always implied. Consecutive superscripts such as ST indicate the nature of the successive derivatives employed to obtain the elastic constant, adiabatic (S) or isothermal (T). For cubic crystals, it can be shown that

$$\gamma_i = \frac{1}{3} (\gamma_i^{11} + \gamma_i^{22} + \gamma_i^{33}) \tag{29}$$

and the explicit expanded form is expressed as

$$\gamma_i = -\left(\frac{1}{6w}\right)\Big[2w + C_{11}{}^{T} + 2C_{12}{}^{T} + (C_{111}+2C_{112})(N_1{}^2U_1{}^2+N_2{}^2U_2{}^2+N_3{}^2U_3{}^2)$$

$$+ (C_{144}+2C_{166})\left[(N_2U_3+N_3U_2)^2 + (N_3U_1+N_1U_3)^2 + (N_1U_2+N_2U_1)^2\right]$$

$$+ 2(C_{123}+2C_{112})(N_2N_3U_2U_3 + N_3N_1U_3U_1 + N_1N_2U_1U_2)\Big] \qquad (30)$$

with

$$w = C_{11}{}^{S}(N_1{}^2U_1{}^2+N_2{}^2U_2{}^2+N_3{}^2U_3{}^2) + C_{44}\left[(N_2U_3+N_3U_2)^2\right.$$

$$\left. + (N_3U_1+N_1U_3)^2 + (N_1U_2+N_2U_1)^2\right] + 2C_{12}{}^{S}(N_2N_3U_2U_3 + N_3N_1U_3U_1$$

$$+ N_1N_2U_1U_2) \quad . \qquad (31)$$

The components of $\underline{N}$ and $\underline{U}$ refer to the appropriate vectors for the i^{th} normal mode, and the elastic constants are expressed in the contracted notation. All third order constants are of the type ST.

The mode Grüneisen parameters for aluminum were calculated as follows: There exist one longitudinal-like and two transverse-like elastic waves for a given direction $\underline{N}$. The effective elastic constants w and, hence, the polarization vectors $\underline{U}$ of these waves can be conveniently determined by solving the elastic wave equation in the form of Quimby and Sutton.[28] The γ_i can then be calculated for any mode using Eqs. (30) and (31) and values of the second and third order elastic constants. The γ_H and γ_L can then be calculated from Eqs. (22) and (23). In computing these sums it is sufficient to consider propagation

directions in a [100] - [110] - [111] triangle on the Debye sphere because of the high symmetry apparent in Eqs. (30) and (31). A grid over this triangle dividing it into 177 nearly equal areas and having evaluation points at the centers of these areas was constructed. This means that 25,488 modes were considered. Results for γ_H and γ_L calculated from our measured values of the third order elastic constants (Table 8) are presented in the first column of Table 10.

An alternate procedure for calculating Grüneisen parameters based directly on Eq. (21) has been developed by Schuele.[29] For cubic crystals, this formulation must be entirely equivalent to the one described here, but the calculations are quite different. Use of both procedures provides a convenient check on the computations of each. Use of the Schuele program and our pressure derivatives (Table 9) gave the same results as our program expressed explicitly in terms of the third order constants. Schuele's program was also used to calculate γ_H and γ_L from the pressure derivatives of Schmunk and Smith[6] (Table 9). These results are presented in the second column of Table 10.

We also computed γ_H and γ_L from the measured thermal properties according to Eq. (20). For γ_H, thermal values were taken at 25°C. The particular values used were as follows: the thermal expansion of Taylor et al.[20] ($\beta = 0.702 \times 10^{-4}$ °C^{-1}), the bulk modulus measured here ($B_S = 0.7585 \times 10^{12}$ dyn·cm^{-2}), the molar volume from the x-ray lattice parameter data of Figgens et al.[30] ($V = 10.004$ cm^3 per mole), and the specific heat of Giaque and Meads[31] ($C_P = 24.34 \times 10^7$ erg. °C^{-1} per mole). The γ_H computed from these values is presented in the third column of Table 10.

At low temperatures, contributions to the thermal expansion and the heat capacity arise from both the lattice and the electron gas. Equation (20) can be separated in the form[32]

$$\gamma = \frac{1}{C_P} \left(C_\ell \gamma_\ell + C_e \gamma_e \right)$$

with (32)

$$\gamma_\ell = \beta_\ell B_S V / C_\ell \ , \quad \gamma_e = \beta_e B_S V / C_e \ .$$

Here sub-ℓ refers to the lattice, and sub-e to the electron gas. We must compute $\gamma_\ell = \gamma_L$ as it is this quantity which is calculated from the elastic data. At low temperatures, the thermal expansion and the heat capacity depend on the temperature as[33]

$$\beta \text{ (or } C) = AT + BT^3 \ . \tag{33}$$

The linear term in temperature is a measure of the electron gas contribution. The cubic term in temperature is a measure of the lattice contribution, and this term must be isolated. The particular values used were as follows: the thermal expansion of White as reported by Collins and White[33] ($(\beta/T^3) = 2.6 \times 10^{-11}$ °C^{-4}), the bulk modulus at 0°K of Kamm and Alers[19] ($B = 0.7938 \times 10^{12}$ dyn·cm^{-2}), the molar volume from the lattice parameter data of Figgens et al.[30] extrapolated to 0°K (V=9.8724 cm^3 per mole), and the specific heat of Phillips[34] ($(C/T^3) = 2.486 \times 10^2$ ergs. °C^{-4} per mole). The γ_L computed from these values is also presented in column 3 of Table 10.

There are two comparisons of interest in Table 10, the absolute magnitudes and the dispersion $(\gamma_H - \gamma_L)$. The continuum model should give excellent agreement between the elastic and thermal values of γ_L.

Table 10. The thermodynamic Grüneisen parameters of Aℓ.

	From elastic data: This Experiment	From elastic data: Schmunk and Smith[67]	From thermal data:
γ_H	2.27	2.56	2.19
γ_L	2.33	2.60	2.45

Unfortunately, the comparison for γ_L is difficult to assess due to large uncertainties (approximately 10%) in the measured thermal expansion. Agreement for γ_H should be questionable as the high frequency lattice modes must be considered. However, results for noble metals[23,35] show that good agreement is obtained between elastic and thermal values of γ_H. If this agreement could be expected for close packed metals in general, the values of γ_H in Table 10 would favor our elastic data versus that of Schmunk and Smith.[6] With regard to the dispersion $(\gamma_H - \gamma_L)$, Barron[36] has shown that for a cubic, close-packed lattice with central forces between nearest neighbors only, $(\gamma_H - \gamma_L) = 0.30$. Also, this difference becomes smaller when more distant neighbors must be taken into account. Measurements by Carr et al.[37] for Cu agree closely with this result. They obtain $(\gamma_H - \gamma_L) = 0.28$ from thermal data. Elastic data will give $(\gamma_H - \gamma_L) = 0.20$. This is consistent with the observation of Hiki and Granato[14] that the elastic properties of the noble metals are determined primarily by the exchange repulsion between ion cores. In aluminum, the elastic properties are determined primarily by the conduction electrons. Hence, one would expect that in a force constant picture distant neighbors would be of major importance. It is interesting to observe in Table 10 that both the thermal and elastic Grüneisen parameters give $(\gamma_H - \gamma_L) < 0$.

V. FORMALISM OF ELASTIC CONSTANT CALCULATIONS

At T = 0°K and in the absence of zero-point vibrations, the elastic constants of a solid have a well defined relationship to the lattice energy. This has been discussed previously (Eq. (9)) but can be simply restated as

$$C_{ijklmn..} = \rho_o \left(\frac{\partial^n E}{\partial \eta_{ij} \, \partial \eta_{kl} \, \partial \eta_{mn} \, ..} \right) . \qquad (34)$$

Here E can be defined simply as a lattice energy per unit mass and is a function of strain only. At T = 0°K, we need not distinguish between an internal and a free energy or between an adiabatic and isothermal elastic constant. Equation (34) can be considered as a basis for elastic constant calculations in terms of atomic models of lattice cohesion.

The elastic constants of Eq. (34) are those which have been defined by Brugger.[2] A calculation in which these quantities are computed directly would be categorized as a finite strain formulation. A finite strain calculation would begin with a description of the lattice energy in terms of volume and interparticle separation, $E = E(V,\underline{r})$. Since V and $\underline{r}$ are known functions of the Lagrangian strain tensor components η_{ij}, the derivatives of Eq. (34) could be set up in terms of a simple chain rule. In any theory of atomic cohesion, the lattice energy is written as a sum of terms, $E = E_1 + E_2 + \ldots$. Although certain of these terms may make a negligible contribution to the cohesive energy, the higher strain derivatives may still be large. In a finite strain approach, it is necessary to analyze all possible contributions to the lattice energy and make a consistent estimate of the dependence of each term on the Lagrangian

strain parameters. The finite strain approach has been used by Ghate[38] to calculate the elastic constants of numerous alkali halides, and by Keating[39] for calculations on the diamond structure.

An alternative formulation for the calculation of elastic constants from atomic models has been presented by Fuchs.[40,41] Fuchs constructed two shear deformations for which the volume was strictly conserved. Each deformation could be expressed in terms of a single parameter. For a cubic crystal, the lattice energy derivatives with respect to these deformation parameters were related directly to the two elastic shear constants $C' = C_{11} - C_{12}$ and C_{44}. The Fuchs approach is based on the assumption that the lattice energy can be written in the form

$$E = E_1(x, \nu) + E_2(\nu \text{ only}) \ . \tag{35}$$

Here x describes a volume conserving deformation, and ν is the relative volume change (V/V_o). The advantage of the Fuchs approach is that the energy term E_2 need not be considered in the calculation of the above mentioned elastic shear constants. It is to be emphasized that this would not be true in an explicit finite strain approach.

The Fuchs approach is particularly convenient in calculations for metals for which the energy decomposition of Eq. (35) can be accomplished in a reasonable manner. In fact, it turns out that, for metals, the energy terms which depend primarily on volume are the most difficult to calculate. For example, for monovalent metals, the wave function of the lowest conduction electron state is known to be very flat in the region between the ions. The energy of this state should depend primarily on volume and be relatively unaffected by a shear distortion of the lattice. The

volume dependence would be given in a complicated way by a quantum mechanical description of electron states. In calculating the elastic shear constants in the approach of Fuchs, such a term can be conveniently neglected. A further discussion of these considerations has been given by Huntington.[42]

The original work of Fuchs[40,41] concerned the calculation of the second order elastic shear constants of the alkali metals and Cu. These calculations were extended to polyvalent metals by Leigh[43] who calculated the second order elastic constants of Al. Leigh's work will be extensively discussed in the following section. The Fuchs approach has also been applied to the second order elastic shear constants of beta brass,[44] Mg,[45] and alpha phase Cu and Ag alloys.[46] Attempts have also been made to explain the pressure derivatives of the second order elastic shear constants of the alkali metals,[7-9] the noble metals,[5] and Al and Mg.[6]

Calculated values of elastic shear constants are of interest because they can be compared to accurately measured quantities. This gives a valuable opportunity to obtain information on application of the theories of interatomic forces. The work of Fuchs has provided two quantities for such comparison for cubic crystals, the two second order elastic shear constants.

Cousins[47] has extended the Fuchs approach to third order for cubic crystals. By considering a general volume conserving shear deformation, he has shown that there are exactly three third order elastic shear constants. He was able to obtain three appropriate deformations which isolated these three third order shear constants. The work of Cousins has provided five quantities for comparison between theory and experiment, the two second and three third order elastic shear constants.

However, a complete extension of the Fuchs approach to the third order for cubic crystals must produce seven independent energy derivatives. That is, to the third order, there are seven independent quantities which can be obtained from consideration of the energy term $E_1(x,\nu)$ alone. The two new quantities which we will consider are effectively volume derivatives of the second order shear constants. The presence of a single derivative with respect to x will eliminate contributions from energy terms of the type E_2. The existence of seven independent quantities related to E_1 alone can be explained in an alternate way. Altogether, for cubic crystals, there must be nine independent energy derivatives, the three second order and six third order Brugger elastic constants. But in eliminating the effect of energy terms $E_2(\nu)$, we eliminate only the second and third energy derivatives with respect to ν. Hence, seven quantities remain.

The Fuchs approach and the finite strain approach are related through the strain dependence of the lattice energy. It is always convenient to express this elastic strain energy in terms of Lagrangian strain parameters and Brugger elastic constants. The energy derivatives with respect to volume conserving shear parameters can then be expressed in terms of a linear combination of Brugger elastic constants. The explicit form of the elastic strain energy for cubic crystals is presented in Appendix B.

We have determined the seven independent energy derivatives of a third order Fuchs approach for cubic crystals in a consistent fashion. The seven derivatives are expressed in terms of linear combinations of the second and third order Brugger elastic constants.

We have used the precedure of Murnaghan.[48] The finite Lagrangian strain tensor can be written in the form

$$\eta_{ij} = \frac{1}{2}(\alpha_{ik}\alpha_{jk} - \delta_{ij}) \tag{36}$$

where

$$\alpha_{ik} = \frac{\partial r_i}{\partial a_k} \quad , \quad \delta_{ij} = \begin{matrix} 0 & i \neq j \\ 1 & i = j \end{matrix} \quad . \tag{37}$$

Here a_k and r_i are cartesian components of the initial and final coordinate vectors $\underline{a}$ and $\underline{r}$, respectively. The above definition of the Lagrangian strain tensor is completely identical to that of Eq. (7). The deformation tensor can be constructed to describe a volume conserving shear deformation, $\alpha_{ik}(x)$, or a simple volume change, $\alpha_{ik}(v)$. Two such deformations can also be combined to produce a shape change (x) and a volume change (v) simultaneously. In this case

$$\alpha_{ik}(x,v) = \alpha_{i\ell}(x)\ \alpha_{\ell k}(v) = v^{1/3}\ \alpha_{ik}(x) \quad . \tag{38}$$

Knowing the deformations $\alpha_{ik}(x,v)$, the Lagrangian strain components $\eta_{ij}(x,v)$ can be obtained from Eq. (36). These can then be substituted into the energy expression (Appendix B) and the derivatives with respect to x and v obtained directly in terms of linear combinations of the Brugger elastic constants. The calculations are lengthy but straightforward and will not be given in detail.

The particular deformations used have been chosen to distort the lattice along directions of high symmetry. This has proven to be especially convenient in treating the energy of the electron gas. The

first two shear deformations which we utilized (x_1 and x_2) are structurally equivalent to those used by Cousins. The third deformation (x_3) has been constructed to produce a deformed lattice of higher symmetry than the third deformation of Cousins. The functional dependence $\alpha_{ik}(x)$ will also be different than that of Cousins for two reasons. First, Cousins (and Fuchs) express their deformations in terms of a parameter x which approaches zero at equilibrium. However, this is only convenient if it becomes necessary to construct a series expansion in terms of x. This is not required in our treatment, and we found that the calculations are simpler when expressed in terms of a parameter which approaches unity at the equilibrium configuration. Also, we found it convenient to construct the deformations in such a way that the $\alpha_{ik}(x)$ can be obtained, one from another, by similarity transformations in terms of the crystal coordinate axes.

The first deformation (x_1) contracts the lattice along the [001] direction and expands it in the plane perpendicular to this direction so as to maintain constant volume. The deformation is described in detail in Appendix C. Applying the procedure of Murnaghan[48] we obtain the following relations:

$$\rho_o \left.\frac{\partial^2 E}{\partial x_1^2}\right|_0 = \frac{4}{3} C' \quad , \tag{39}$$

$$\rho_o \left.\frac{\partial^3 E}{\partial x_1^3}\right|_0 = -\frac{20}{3} C' - \frac{2}{9}(C_{111}-3C_{112}+2C_{123}) \quad , \tag{40}$$

$$\rho_o \left.\frac{\partial^3 E}{\partial \nu \partial x_1^2}\right|_0 = \frac{4}{9}(3B+4C') + \frac{2}{9}(C_{111}-C_{123}) \quad . \tag{41}$$

The second deformation (x_2) contracts the lattice along the [111] direction and expands it in the plane perpendicular to this direction so as to maintain constant volume. If we let R_{mi} be the transformation which rotates the [001] axis into the [111] axis, then this deformation can be obtained from the first by the similarity transformation

$$\alpha_{mn}(x_2) = R_{mi}R_{kn}\alpha_{ik}(x_1) \quad .$$

The deformation is described in detail in Appendix C. We obtain the following relations:

$$\rho_o \left.\frac{\partial^2 E}{\partial x_2^{\,2}}\right|_0 = \frac{4}{3} C_{44} \quad , \tag{42}$$

$$\rho_o \left.\frac{\partial^3 E}{\partial x_2^{\,3}}\right|_0 = -\frac{20}{3} C_{44} - \frac{16}{9} C_{456} \quad , \tag{43}$$

$$\rho_o \left.\frac{\partial^3 E}{\partial \nu \partial x_2^{\,2}}\right|_0 = \frac{4}{9}(3B+4C_{44}) + \frac{4}{9}(C_{144}+2C_{166}) \quad . \tag{44}$$

The third deformation (x_3) contracts the lattice along the [110] direction and expands it in the plane perpendicular to this direction so as to maintain constant volume. It can also be obtained by a similarity transformation from (x_1) as shown above. The deformation is described in detail in Appendix C. We obtain the following relations:

$$\rho_o \frac{\partial^2 E}{\partial x_3^2}\bigg|_0 = \frac{1}{3}(C'+3C_{44}) \ , \tag{45}$$

$$\rho_o \frac{\partial^3 E}{\partial x_3^3}\bigg|_0 = -\frac{5}{3}(C'+3C_{44}) + \frac{1}{36}(C_{111}-3C_{112}+2C_{123}) - (C_{166}-C_{144}) \ , \tag{46}$$

$$\rho_o \frac{\partial^3 E}{\partial v \partial x_3^2}\bigg|_0 = \frac{1}{3}(4B+\frac{4}{3}C'+4C_{44}) + \frac{1}{18}(C_{111}-C_{123}) + \frac{1}{3}(C_{144}+2C_{166}) \ . \tag{47}$$

In the above relations we have used the notation $C' = \frac{1}{2}C_{11}-C_{12}$ and $B = \frac{1}{3}C_{11} + \frac{2}{3}C_{12}$. Note in the above that Eq. (45) is a linear combination of Eqs. (39) and (42). Also, Eq. (47) is a linear combination of Eqs. (41) and (44). Thus, Eqs. (45) and (47) will provide no new information but are convenient for the purpose of checking explicit calculations.

If an isotropic crystal is mistakenly analyzed as if it were cubic, certain relations must exist among the cubic elastic constants. In particular, for the second order constants, we have the well known relation

$$C' = C_{44} \ . \tag{48}$$

In the third order, there are three relations among the six elastic constants. These can be written

$$C_{456} = (1/2)(C_{166} - C_{144}) \ , \tag{49}$$

$$C_{456} = (1/8)(C_{111} - 3C_{112} + 2C_{123}) \ , \tag{50}$$

$$C_{144} + 2C_{166} = (1/2)(C_{111} - C_{123}) \ . \tag{51}$$

Also, since the three deformations above can be obtained, one from another, by similarity transformations, the respective Fuchs-type derivatives should be identical if the solid were isotropic. Combining Eqs. (48) - (51) with Eqs. (39) - (47), we see that this is exactly the case.

The seven independent Fuchs relations, Eqs. (39) - (44) and (46), can be recombined in linear combinations which are convenient to compare to experimental results. These relations are presented in Table 11, and will be utilized in this form in the following section.

As stated previously, in any elastic constant formulation to the third order for cubic crystals, there must be nine independent energy derivatives. In the Fuchs approach, we consider only the seven derivatives discussed above and summarized in Table 11. For completeness, we will mention the two energy derivatives that have been neglected here. These are

$$\rho_o \frac{\partial^2 E}{\partial v^2}\bigg|_0 = B \tag{52}$$

$$\rho_o \frac{\partial^3 E}{\partial v^3}\bigg|_0 = -B + \frac{1}{9}(C_{111}+6C_{112}+2C_{123}) \; . \tag{53}$$

These derivatives would explicitly involve energy terms of the type E_2 and would be more difficult to compute from atomic models of metallic cohesion than the Fuchs derivatives.

Table 11. The seven independent Fuchs relations to the third order for cubic crystals. This form is particularly convenient for comparison to measured quantities.

Elastic Constant	Fuchs Energy Derivative
c'	$\frac{3}{4}\rho_o \left.\frac{\partial^2 E}{\partial x_1^2}\right\|_o$
c_{44}	$\frac{3}{4}\rho_o \left.\frac{\partial^2 E}{\partial x_2^2}\right\|_o$
$\frac{1}{8}(c_{111} - 3c_{112} + 2c_{123})$	$-\frac{9}{16}\rho_o \left.\frac{\partial^3 E}{\partial x_1^3}\right\|_o - \frac{45}{16}\rho_o \left.\frac{\partial^2 E}{\partial x_1^2}\right\|_o$
c_{456}	$-\frac{9}{16}\rho_o \left.\frac{\partial^3 E}{\partial x_2^3}\right\|_o - \frac{45}{16}\rho_o \left.\frac{\partial^2 E}{\partial x_2^2}\right\|_o$
$\frac{1}{2}(c_{166} - c_{144})$	$-\frac{1}{2}\rho_o \left.\frac{\partial^3 E}{\partial x_3^3}\right\|_o - \frac{1}{16}\rho_o \left.\frac{\partial^2 E}{\partial x_1^2}\right\|_o - \frac{15}{16}\rho_o \left.\frac{\partial^2 E}{\partial x_1^2}\right\|_o - \frac{15}{8}\rho_o \left.\frac{\partial^2 E}{\partial x_2^2}\right\|_o$

Table 11 (continued)

Elastic Constant	Fuchs Energy Derivative
$3B + \frac{1}{2}(C_{111} - C_{123})$	$\frac{9}{4}\rho_o \left.\frac{\partial^3 E}{\partial \nu \partial x_1^2}\right\|_o - 3\rho_o \left.\frac{\partial^2 E}{\partial x_1^2}\right\|_o$
$3B + (C_{144} + 2C_{166})$	$\frac{9}{4}\rho_o \left.\frac{\partial^3 E}{\partial \nu \partial x_2^2}\right\|_o - 3\rho_o \left.\frac{\partial^2 E}{\partial x_1^2}\right\|_o$

VI. A CALCULATION OF THE ELASTIC CONSTANTS OF Aℓ

Leigh[43] has calculated the second order elastic shear constants of Al using a Fuchs approach. We have extended this theory to the third order to see whether it would explain the measured third order elastic constants.

Leigh's calculation was based on a Wigner-Seitz[49,50] decomposition of the lattice energy. The energy terms which must be considered are the kinetic energy of the lowest electronic state, the electrostatic energy, and the Fermi energy (here we mean the total energy of the Fermi sea and not the energy of the highest filled electron state). The kinetic energy of the lowest electronic state should depend on volume only and can be negelected in a Fuchs calculation of the elastic shear constants. The electrostatic energy, which is a correction term which must be applied to the cell calculation of Wigner-Seitz, was modified to account for the polyvalent nature of Al. The Fermi energy and its appropriate shear derivatives were treated in an empirical way, being expressed in terms of parameters which could, in principal, be obtained from experimental information and from band structure calculations. The calculation was restricted to the Hartree one electron approximation, neglecting the effects of conduction electron exchange and correlated electron motion. The exchange repulsion between ion cores was also neglected. This should be a good approximation for Al.[51]

The important contributions which must be considered in detail are the electrostatic energy and the Fermi energy. For the electrostatic energy, Leigh used a simple modification of the earlier work of Fuchs.[40] Leigh's treatment of the energy of the Fermi sea was analogous to a nearly-free-electron approach. Since Al has three valence electrons, more

than one energy band must be occupied. In a zone picture, the first Brillouin zone has sufficient states for two electrons per atom. The third electron must go into the higher zones. Leigh treated the first and higher zones separately. The energy of the first zone was expressed in terms of an effective mass at the bottom of the band and a parameter to account for the non-parabolic nature of the dependence E(k) at the zone boundaries. The energy of electrons in the higher zones was described in terms of the energies at the zone faces and the density of states at the Fermi surface. Sufficient parameters were available to fit exactly the measured values of the second order elastic shear constants.

At the time of Leigh's calculation (1951) there was only limited knowledge of the Fermi sea parameters from other experiments and calculations. In particular, there was no information available on the energies at the zone faces. This gave Leigh considerable freedom in choosing these parameters. In the past 10 years, extensive information has become available about the Fermi sea from both theory and experiment. The parameters used in Leigh's theory can now be well estimated from other measurements and calculations. It is now possible to consider a quantitative evaluation of Leigh's theory and its extension to the third order elastic constants.

In extending Leigh's theory to the third order elastic constants of Al, we first consider the electrostatic energy. In the method of Wigner and Seitz,[49,50] the lattice is divided into polyhedra centered on atomic sites. The conduction electrons and ionic cores are considered separately. In the simplest form of the theory for monovalent metals, one conduction electron is assigned to each cell to account for correlation effects. The polyhedra are replaced by spheres of equal volume

(and radius r_o), and the energy of the lowest conduction electron state is found by solving the Schroedinger equation using a known ionic potential and the boundary condition $d\psi/dr\big|_{r=r_o} = 0$. The resulting energy is lower than the energy of this electron in the atom, and this is the essence of the metallic bond. In the polyhedra picture, the polyhedra would interact electrostatically. If the sphere approximation were accurate, there would be no interaction. This interaction can be calculated by obtaining the electrostatic energy per atom of the actual lattice and subtracting off the self energy of the sphere. Although this is a small correction to the cohesive energy, it is a sensitive function of lattice configuration and makes an important contribution to the elastic shear constants.

Fuchs[40] calculated how this electrostatic energy term contributes to the second order elastic shear constants. Cousins[47] repeated this calculation and extended it to the third order elastic shear constants. His results for the second order constants agreed with Fuchs to within $\pm$ 0.1%. These results are presented in Table 12. We also require the electrostatic contribution to the energy derivatives that describe the volume dependence of the second order shear constants. These can be calculated directly from the relations given by Cousins. As a particular example we consider the second order shear constant C'. From the first rows of Tables 11 and 12 we have

$$C'_{el} = (3/4)\,\rho_o(\partial^2 E_{el}/\partial x_1^2)\big|_o = 48.81\,(Z^2/a^4) \quad . \qquad (54)$$

The volume dependence of the second energy derivative in Eq. (54) can be written as

$$\rho_o(\partial^2 E_{el}/\partial x_1^2) = (4/3) \times 48.81\,(Z^2/a^4)\; v^{-1/3} \quad . \qquad (55)$$

Hence, the mixed third derivative is given by

$$\rho_o(\partial^3 E_{el}/\partial v \partial x_1^2)\big|_o = (-1/3)(4/3)\, C'_{el} \quad . \tag{56}$$

From the sixth row of Table 11, we have that

$$\begin{aligned}(3B + \tfrac{1}{2}(C_{111} - C_{123}))_{el} &= (9/4)(-4/9)C'_{el} - 3(4/3)C'_{el} \\ &= (-5)C'_{el} \quad . \end{aligned} \tag{57}$$

The calculation involving C_{44} is entirely equivalent. The results for the electrostatic contribution to these two energy derivatives are also presented in Table 12. In the above and in Table 12, a is the lattice constant, and Z is an effective valence. The numerical factors are those for units of 10^{11} dyn.cm^{-2} with a in angstroms.

Hence, we know the contribution of the electrostatic energy to the seven elastic constants summarized in Table 11 in terms of an effective valence. In a formulation based on the energy decompoisition of Wigner and Seitz, this effective valence is just a measure of the charge density at the boundary of an atomic polyhedron. For monovalent metals, the effective valence must be very close to unity. For polyvalent Al, the effective valence is not necessarily three. By rearranging terms in the Hartree expression for the total energy of the Al lattice, Leigh determined that the electrostatic contribution to the elastic constants of Al could be simply obtained by utilizing an effective valence which was less than three due to the nonuniformity of the conduction electron distribution. This resulted from an analysis of electron densities in terms of real wave functions. Leigh arbitrarily chose a representative value of $Z^2 = 7.0$.

Table 12. Electrostatic contribution to the elastic constants in a Fuchs formulation for an FCC lattice. (units of $(Z^2/a^4)\ 10^{11}$ dyn.cm^{-2} with a in Å)

Elastic Constant	Electrostatic Contribution
C'	48.81
C_{44}	437.4
$\frac{1}{8}(C_{111} - 3C_{112} + 2C_{123})$	593.1
C_{456}	590.4
$\frac{1}{2}(C_{166} - C_{144})$	- 1342
$3B + \frac{1}{2}(C_{111} - C_{123})$	- 244.05
$3B + (C_{144} + 2C_{166})$	- 2187

In the theory of Leigh, the elastic constants can be obtained from two contributions, the electrostatic energy and the Fermi energy. Using Leigh's value for Z^2 and $a = 4.04\text{Å}$, we can calculate numerical values for the electrostatic contribution. Knowing the measured elastic constant, we can then obtain the Fermi energy contribution by subtraction. Fermi energy contributions obtained in this manner are summarized in Table 13. For the experimental elastic constants, we should use the values appropriate to $T = 0°K$ in the absence of zero-point vibrations. For the second order constants the appropriate values can be obtained by extrapolating the room temperature values (Table 1) linearly to $T = 0°K$ using the measured temperature derivatives (Table 3). Unfortunately, we do not know the temperature variation of the third order constants. We must use the room temperature measured values. We would hope that this would not introduce an error of more than 10%, which should not be serious compared to inaccuracies in the model calculation.

We now consider the extension of Leigh's theory to the third order elastic constants for the Fermi energy contributions. The values calculated here will be compared to those summarized in Table 13. The Fermi energy is considered in two parts, the filled first zone and the higher zones. At the time of Leigh's calculation, it was not known whether or not the first zone was, in fact, completely filled. Now it is known to be so.[52]

To consider the filled first zone, we proceed according to the method of Leigh. The Brillouin zone is the Wigner-Seitz polyhedron of the reciprocal lattice. The reciprocal lattice of FCC is BCC, and the Brillouin zone is the well-known truncated octahedron. Leigh divided the zone into tetrahedra which could be defined by three

Table 13. Separation of the elastic constants of Aℓ into electrostatic and Fermi energy contributions in a Fuchs approach based on a Wigner-Seitz energy decomposition. (units of 10^{11} dyn.cm^{-2})

Elastic Constant	Measured Value	Electrostatic Contribution	Fermi Energy Contribution
C'	2.74	1.28	1.46
C_{44}	3.27	11.49	- 8.22
$\frac{1}{8}(C_{111}-3C_{112}+2C_{123})$	- 0.84	15.58	- 16.42
C_{456}	- 3.00	15.51	- 18.51
$\frac{1}{2}(C_{166}-C_{144})$	- 15.85	- 35.26	19.41
$3B + \frac{1}{2}(C_{111}-C_{123})$	- 31.40	- 6.41	- 24.99
$3B + (C_{144}+2C_{166})$	- 46.10	- 57.47	11.37

vectors: the vector $\underline{p}$ extending from the center of the zone to the center of a face, the vector $\underline{q}$ extending from the center of the face to the midpoint of an edge of the face, and the vector $\underline{r}$ extending from the midpoint of the edge of the face to a corner of the face. The Brillouin zone and one such tetrahedron are illustrated in Fig. 6. There are 144 tetrahedra, 12 based on each hexagonal face and 8 on each square face.

It is next necessary to approximate to the function $E(k)$ for the first zone. Leigh has used the formula

$$E(k) = \frac{\alpha \hbar^2}{2m}\left[k^2 - \lambda \left(p^2 \left(\frac{k'_z}{p}\right)^{2/\lambda} + q^2 \left(\frac{k'_y}{q}\right)^{2/\lambda} + r^2 \left(\frac{k'_x}{r}\right)^{2/\lambda} \right) \right] \tag{58}$$

Here k'_z, k'_y, k'_x are measured along p, q, and r, respectively, for each tetrahedron. α is a measure of the effective mass at the bottom of the band. The parameter λ modifies the otherwise spherical energy surfaces in the region of the zone boundary to cut the zone normally so that the energy at the center of any face is the same fraction $(1-\lambda)$ of the free electron energy. $E(k)$ can now be integrated over a tetrahedron to obtain the total electron energy in that tetrahedron, and the tetrahedra summed over to obtain the first zone contribution to the Fermi energy.

$$E_F{}^I = \frac{\alpha \hbar^2}{(2\pi)^3 m} \sum_{TET} pqr \, (Fp^2 + Gq^2 + Hr^2) \tag{59}$$

with

$$F = \frac{1}{10} - \frac{\lambda^2}{2(2+3\lambda)}, \qquad G = \frac{1}{20} - \frac{\lambda^3}{2(2+3\lambda)(1+\lambda)}$$

$$H = \frac{1}{60} - \frac{\lambda^4}{2(2+3\lambda)(1+\lambda)(2+\lambda)} . \tag{60}$$

Fig. 5. The FCC Brillouin zone and its division into tetrahedral segments. Γ, X, and L represent points of high symmetry. $\underline{p}$, $\underline{q}$, and $\underline{r}$ are the vectors describing a particular tetrahedron.

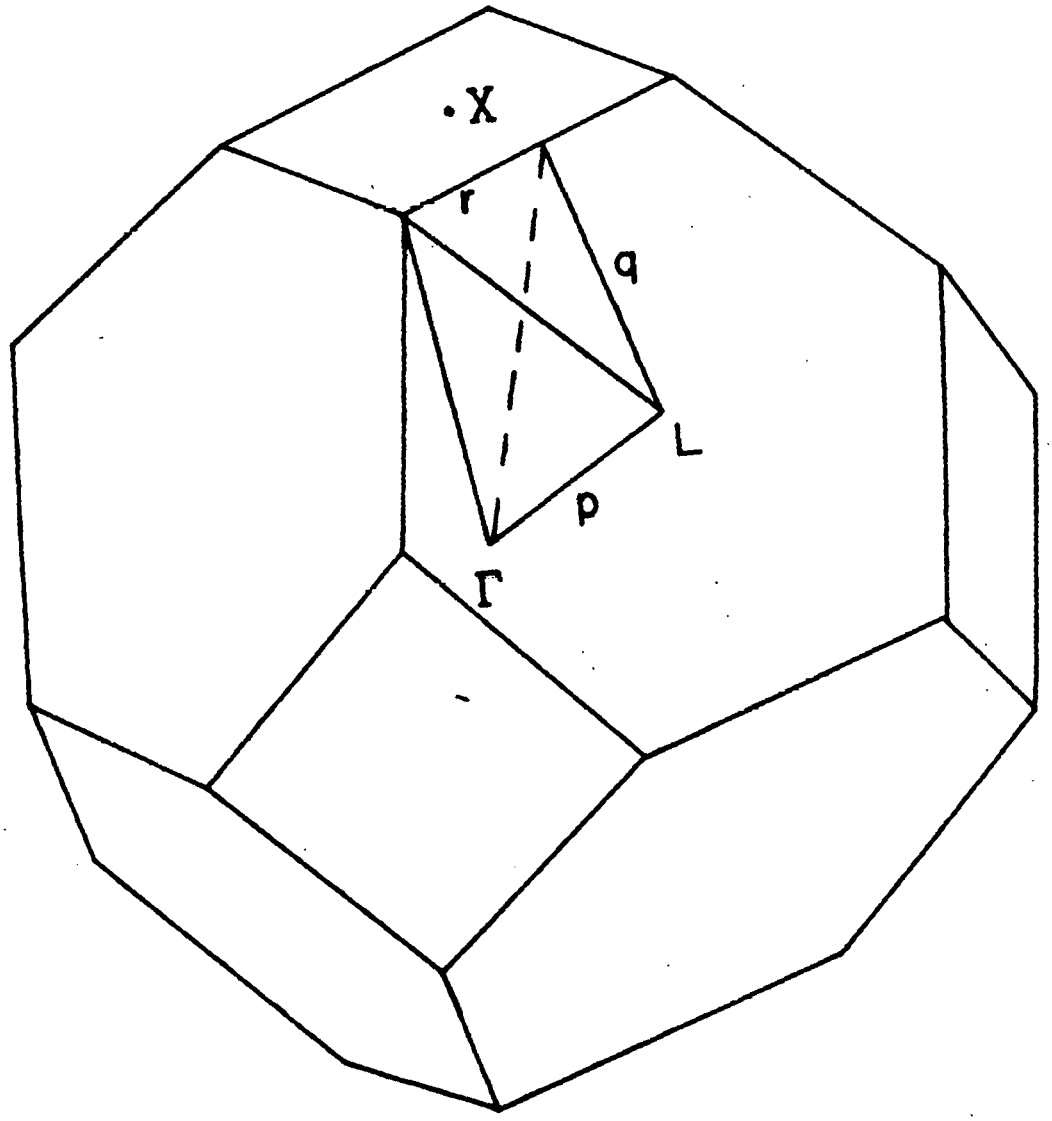
X
r
q
L
p
Γ

We must now calculate the appropriate derivatives of the energy term E_F^I. We know how the basis vectors of the reciprocal lattice change with the three shear deformations which we have defined, x_1, x_2, and x_3. This has been summarized in Appendix C. Hence, we can calculate how the vectors $\underline{p}$, $\underline{q}$, and $\underline{r}$ for each tetrahedron change with each deformation. This is an involved and complicated procedure. One must first construct the Brillouin zone of the strained reciprocal lattice from the transformed basis vectors. Only then can the $\underline{p}(x)$, $\underline{q}(x)$, and $\underline{r}(x)$ be obtained for each tetrahedron. These vectors will not change by the same transformation as the basis vectors. The results for each deformation can be checked by calculating the volume of the zone which must be independent of x. In performing these calculations, there will be six different tetrahedra for x_1, five for x_2, and ten for x_3. Knowing the dependence of the vectors $\underline{p}$, $\underline{q}$, and $\underline{r}$ on the strain parameters, we can calculate the second and third energy derivatives with respect to these strain parameters and, hence, the appropriate contributions to the elastic constants. It turns out that the dependence on λ is very slight (generally less than 2% for $\lambda = 0.1$), and we can make the numerical approximation $\lambda = 0$. The results are presented in column 2 of Table 14 in terms of the free electron energy at the X symmetry point of the Brillouin zone

$$E_X = \frac{\alpha \hbar^2}{2m} \left(\frac{2\pi}{a}\right)^2 \tag{61}$$

where a is the lattice constant.

In column 2 of Table 14, the expression for the first zone contribution to C' and C_{44} are the same as those of Leigh. For C' this must be the case as we have used identical strain parameters. For C_{44}, our

deformation is structurally equivalent although algebraically different from that of Leigh. Hence, we must still obtain the same result for the elastic constant contribution. The other entries in this column constitute our extension to the third order of this part of Leigh's calculation.

The contribution to the elastic constants from the energy of the electrons in the higher zones will also be calculated according to the method of Leigh. The treatment will effectively consider second zone regions only. We neglect explicit consideration of the electrons in the third zone. It is known from an extensive analysis of de Haas - van Alphen measurements[53] that only a small fraction of 1 electron/atom is in the third zone (near the first zone edges), and the fourth zone (near the first zone corners) is empty.

After Leigh, we let $N_i(E-E_{ij})$ be the number of electron states including spin degeneracy per atom per unit energy at energy E above energy E_{ij} at the center of the j^{th} pair of the i^{th} type face (hexagonal or square) in the second zone. Then the number of electrons n_{ij} in the second zone region (ij) is given by

$$n_{ij} = \int_{E_{ij}}^{\zeta} N_i(E-E_{ij})dE = \int_{o}^{\zeta-E_{ij}} N_i(\epsilon)d\epsilon \ . \qquad (62)$$

Here ζ is the Fermi level. Using the same notation for the division of the energy, we can write

$$W_{ij} = \int_{E_{ij}}^{\zeta} N_i(E-E_{ij})E \ dE = n_{ij}E_{ij} + \int_{o}^{\zeta-E_{ij}} N_i(\epsilon)\epsilon \ d\epsilon \ . \qquad (63)$$

For any of the three strain parameters x we have

$$\frac{dn_{ij}}{dx} = N_i(\zeta - E_{ij}) \left(\frac{d\zeta}{dx} - \frac{dE_{ij}}{dx} \right) . \tag{64}$$

But it is assumed that the first zone is full and stays full during any deformation, therefore

$$\sum_{ij} n_{ij} = 1 , \tag{65}$$

and the summed strain derivatives of any order of n_{ij} are identically zero. From this fact and Eq. (64), we determine that

$$\left. \frac{d\zeta}{dx} \right|_o = 0 . \tag{66}$$

This is a consequence of the fact that the volume remains constant during the deformations x.

From Eq. (63), the second strain derivatives of each contribution to the second zone energy are given by

$$\left. \frac{d^2W_{ij}}{dx^2} \right|_o = n_{ij} \left. \frac{d^2E_{ij}}{dx^2} \right|_o - N_i(\zeta - E_{ij}) \left(\left. \frac{dE_{ij}}{dx} \right|_o \right)^2 + \zeta \left. \frac{d^2n_{ij}}{dx^2} \right|_o . \tag{67}$$

Equation (67) can be summed over the regions (ij). Using Eq. (65) we obtain

$$\left. \frac{d^2E_F^{II}}{dx^2} \right|_o = \sum_{ij} \left. \frac{d^2W_{ij}}{dx^2} \right|_o = \sum_i \left[n_i \sum_j \left. \frac{d^2E_{ij}}{dx^2} \right|_o - N_i(\zeta - E_{ij}) \sum_j \left(\left. \frac{dE_{ij}}{dx} \right|_o \right)^2 \right] \tag{68}$$

This result is given by Leigh. From Eq. (67), we can obtain the third strain derivatives of the second zone energy contributions in a straightforward manner. Again using Eqs. (65) and (66) and summing over the regions (ij), we obtain the result

$$\left.\frac{d^3E_F^{II}}{dx^2}\right|_o = \sum_{ij}\left.\frac{d^3W_{ij}}{dx^3}\right|_o = \sum_i \left[n_i \sum_j \left.\frac{d^3E_{ij}}{dx^3}\right|_o - 3N_i(\zeta - E_{ij}) \sum_j \left.\frac{dE_{ij}}{dx}\right|_o \left.\frac{d^2E_{ij}}{dx^2}\right|_o \right] \tag{69}$$

In Eq. (69) we have neglected a term proportional to the strain derivative of the density of states at the Fermi surface. For a nearly-free-electron metal, the density of states at the Fermi surface should depend only on the Fermi level. Hence, by Eq. (66), the density of states should not change with strain to the first order.

From Eq. (67) we can also obtain the mixed third derivatives of the second zone energy contributions. Here we encounter a term proportional to the volume derivative of the density of states at the Fermi surface. This must be included. Summing over the regions (ij) we obtain

$$\left.\frac{d^3E_F^{II}}{d\nu dx^2}\right|_o = \sum_{ij}\left.\frac{d^3W_{ij}}{d\nu dx^2}\right|_o = \sum_i \left[n_i \sum_j \left.\frac{d^3E_{ij}}{d\nu dx^2}\right|_o \right.$$

$$\left. - 2N_i(\zeta - E_{ij}) \sum_j \left.\frac{dE_{ij}}{dx}\right|_o \left.\frac{d^2E_{ij}}{d\nu dx}\right|_o - N_i(\zeta - E_{ij}) \frac{d \ln N}{d\nu} \sum_j \left(\left.\frac{dE_{ij}}{dx}\right|_o \right)^2 \right] \tag{70}$$

The form of the last term in Eq. (70) assumes that each of the $N_i(\zeta-E_{ij})$ have the same volume dependence. In Eq. (70) we have neglected a term proportional to dn_{ij}/dv. Such a factor would depend on the change in the energy gaps at the zone boundary with volume. This dependence is non-zero and has been measured.[54] However, the effect is of higher order than one that should be included in a nearly-free-electron model and, hence, has not been considered.

Equations (68)-(70) describe the contribution of the energy of the electrons in the higher zones to the elastic constants in terms of general deformation parameters. We must now compute the respective energy derivatives for the deformations used here. Leigh made the assumption that the energies E_{ij} varied as p_{ij}^2, where p_{ij} is the vector from the center of the zone to the center of the face bounding region (ij). We retain that assumption here. The p_{ij} are simply the $\underline{p}$ vectors which were considered in the first zone calculation. We know the dependence of these vectors on the strain parameters x_1, x_2, x_3, and v, and we can calculate the energy derivatives of Eqs. (68)-(70) for each of the three deformations. The energy derivatives will be given simply by the respective energy E_{ij} multiplied by a numerical factor.

The results are presented in Table 14. Here, E_X and E_L represent the energies at the X and L symmetry points at the square and hexagonal faces, respectively. Similarly, n_X and n_L are the number of electrons per atom overlapping the square and hexagonal faces, respectively, subject to the condition

$$3n_X + 4n_L = 1 \quad . \tag{71}$$

N_X and N_L are the density of states at the Fermi level in the respective

regions subject to the condition

$$3N_X + 4N_L = N \quad . \tag{72}$$

Here N is the measured density of states at the Fermi level. If we recall that N is a density of states per atom, it follows that d ln N/dv is simply the electronic Grüneisen parameter as described in the section IV. In Table 14, rows 1 and 2 correspond to Eq. (68), and these are the results for the Fermi energy contributions to the second order elastic shear constants given by Leigh. Rows 3-5 correspond to linear combinations of Eqs. (68) and (69), and rows 6 and 7 to linear combinations of Eqs. (68) and (70). These entries constitute our extension to the third order of Leigh's Fermi energy calculation.

The expressions of Table 14 can be used to compute the Fermi energy contributions to the elastic constants in a Fuchs approach. It is now known that the gross electronic structure of Al can be described surprisingly well by a nearly free electron model with a reduced effective mass $\alpha^{-1} = 1.00\ (\pm 0.03)$.[52,53,*] This dictates the choice of numerical values for the parameters of Table 14. We choose the free electron values $E_X = 9.21$ ev and $E_L = 6.91$ ev. Adjustment of these values to account for the band gaps at the zone faces would be a small correction. The number of electrons per atom overlapping a particular pair of faces should be nearly proportional to the volume enclosed between the respective zone face and the free electron sphere. Using this criterion and Eq. (71) we obtain $n_X = 0.041$ and $n_L = 0.219$. The density of states at the Fermi surface over a particular pair of faces should be nearly proportional to the area of the face, hexagonal or square. Using this criterion, Eq. (72), and the measured density of states N = 0.572 per

*N. W. Ashcroft, private communication.

Table 14. Fermi energy contributions to the elastic constants of Aℓ in a Fuchs formulation. (implied units are energy/atom or V_c^{-1}.energy/volume where V_c is the atomic volume)

Elastic Constant	First Zone Contribution	Term 1 Eqs. (68)-(70)	Term 2 Eqs. (68)-(70)	Term 3 Eq. (70)
C'	$\frac{1}{6} E_X$	$(2n_X E_X + \frac{8}{3} n_L E_L)$	$-2N_X E_X^2$	-
C_{44}	$\frac{1}{2} E_X$	$(2n_X E_X + \frac{8}{3} n_L E_L)$	$-\frac{16}{9} N_L E_L^2$	-
$\frac{1}{8}(C_{111}-3C_{112}+2C_{123})$	$\frac{2}{3} E_X$	$-2(2n_X E_X + \frac{8}{3} n_L E_L)$	$6 N_X E_X^2$	-
C_{456}	$-\frac{1}{3} E_X$	$-2(2n_X E_X + \frac{8}{3} n_L E_L)$	$\frac{16}{3} N_L E_L^2$	-
$\frac{1}{2}(C_{166}-C_{144})$	$-\frac{4}{3} E_X$	$-2(2n_X E_X + \frac{8}{3} n_L E_L)$	$-2(N_X E_X^2 + \frac{16}{9} N_L E_L^2)$	-
$3B + \frac{1}{2}(C_{111}-C_{123})$	$-\frac{3}{2} E_X$	$-6(2n_X E_X + \frac{8}{3} n_L E_L)$	$16 N_X E_X^2$	$-6 \frac{d \ln N}{d\nu} N_X E_X^2$
$3B + (C_{144}+2C_{166})$	$-\frac{9}{2} E_X$	$-6(2n_X E_X + \frac{8}{3} n_L E_L)$	$\frac{128}{9} N_L E_L^2$	$-\frac{16}{3} \frac{d \ln N}{d\nu} N_L E_L^2$

ev atom,[34] we obtain $N_X = 0.042$ and $N_L = 0.112$ per ev atom. We also choose the measured value $d \ln N/d\nu = 1.8$ from the low temperature thermal expansion measurement of White as reported by Collins and White.[33] Substituting these values into the expressions of Table 14, we can compute the Fermi energy contributions to the elastic constants in a Fuchs approach. The results are presented in Table 15 and compared to the Fermi energy contributions obtained in Table 13.

The agreement between the two sets of Fermi energy contributions in Table 15 is, to say the least, very bad. The isolated agreement of row 6 should probably not be taken seriously. Although we are involved with the difference of large numbers, with the exception of row 1 the agreement could not be substantially improved by adjustments in the individual terms of even 25%. In any event, the individual terms are not independent, and such adjustments would be quite out of the question.

We have used numerical values consistent with the known nearly-free-electron behavior of Al. At the time of Leigh's calculation, this behavior was not appreciated. It is only recently that the development of the pseudopotential approach gave theoretical justification for the nearly-free-electron picture.[55] Leigh's ability to fit the second order shear constant Fermi energy terms depended largely on his choice of $E_L = 9.08$ ev. This is more than 30% higher than the free electron value and is not an acceptable choice. Leigh's values for this and the other parameters were based on his assumption that only small, isolated pockets of electrons existed in the higher zones. The analysis was more nearly appropriate for a semiconductor than a nearly-free-electron metal. It might still be noted, however, that use of Leigh's values for the Fermi energy parameters would not produce general agreement

Table 15. Fermi energy contributions to the elastic constants in a Fuchs approach according to the method of Leigh. Term 1, Term 2, and Term 3 refer to the higher zone contributions of Eqs. (68)-(70). The values presented in column 7 are those calculated from the difference of the measured constants and the electrostatic contributions. (units of 10^{11} dyn.cm^{-2} obtained using an atomic volume of 16.48 A^3)

Elastic Constant	First Zone	Term 1	Term 2	Term 3	Total Col. 2-5	By Difference
C'	1.49	4.66	- 6.93	-	- 0.78	1.46
C_{44}	4.48	4.66	- 9.24	-	- 0.10	- 8.22
$\frac{1}{8}(C_{111}-3C_{112}+2C_{123})$	5.97	- 9.32	20.78	-	17.43	-16.42
C_{456}	- 2.99	- 9.32	27.73	-	15.42	-18.51
$\frac{1}{2}(C_{166}-C_{144})$	-11.94	- 9.32	25.41	-	4.15	19.41
$3B + \frac{1}{2}(C_{111}-C_{123})$	-13.43	-27.95	55.42	-37.41	-23.37	-24.99
$3B + (C_{144}+2C_{166})$	-40.29	-27.95	73.94	-49.91	-44.21	11.37

between the two sets of Fermi energy contributions.

We conclude that numerical adjustments in Table 15 will not substantially improve the Fermi energy calculation. The model must be defective. Although the gross electronic structure of Al is close to a nearly-free-electron model, the detailed structure near the zone boundaries is, of course, much more complicated.[53] Although the energy differences involved are small, the energy changes with deformation must be large. It was our decision that the method of Leigh could only be extended to the third order in the nearly-free-electron approximation. Thus, we neglected the geometrical considerations of the third zone regions. We conclude that the second and third derivatives of the complicated energy band structure near the first zone edges and corners must be important in the calculation of the elastic constants of Al.

Schmunk and Smith[6] have used the Leigh method to attempt to explain the pressure derivatives of the second order elastic shear constants of Al. They were forced to assume that the effective valence varied with volume in order to compute values of these two quantities in agreement with experiment. However, the inclusion of a term modifying the electrostatic energy contribution cannot eliminate all the discrepancies in Table 15. A volume dependence of the effective valence would not be included in a calculated third order shear constant where we consider strictly volume conserving deformations. Any attempt to rescue the Leigh procedure would require modifications of the Fermi energy contribution.

Work now in progress at the University of Illinois has indicated that a pseudopotential approach might be applicable to the calculation of the elastic constants of the alkali metals.[*] The pseudopotential

---

*T. Suzuki, private communication.

approach should also be applicable to Al. The structure of Al can be accounted for qualitatively in terms of pseudopotential parameters.[56] It does not seem worthwhile to further pursue the Leigh method for the calculation of the elastic constants of Al. Rather, it is suggested that a pseudopotential calculation be attempted.

VII. CONCLUSIONS

The complete set of six third order elastic constants of single crystal Al has been experimentally determined by measuring both hydrostatic pressure and uniaxial stress derivatives of the natural sound velocities using a two specimen interferometric technique. The specimens were neutron irradiated to eliminate dislocation effects from the uniaxial experiments. A self-consistent set of hydrostatic pressure derivatives of the second order elastic constants has been calculated from the measured third order elastic constants. The third order elastic constants have also been used to calculate the thermal expansion in the anisotropic continuum model at both high and low temperatures, and a comparison has been made to the directly measured expansion coefficients.

The seven independent relations between second and third order elastic constants and appropriate lattice energy derivatives in a Fuchs approach have been obtained. The related deformation parameters have been described in a consistent fashion. The applicability of the Fuchs approach to elastic constant calculations for metal crystals has been discussed in terms of the neglect of energy terms which depend upon volume only.

An attempt has been made to calculate the second and third order elastic constants of Al in a Fuchs approach using a Wigner-Seitz decomposition of the lattice energy. The terms considered were the electrostatic energy and the Fermi energy. The Fermi energy was treated in a nearly-free-electron approximation. The fact that this attempt

was unsuccessful has been attributed to the complicated energy band structure of Al in the vicinity of the Brillouin zone boundaries.

APPENDIX A

The calculation of Espinola and Waterman[13] can be modified to account for an initial phase difference between the two sound waves. We assume that a cosine wave is propagated in each specimen. We neglect the attenuation and the finite length of the pulse. Let

$$\begin{aligned} A_1 &= A_o \cos(\omega t - k_1 x_1) \\ A_2 &= A_o \cos(\omega t - k_2 x_2 + \varphi) \quad . \end{aligned} \tag{A1}$$

These waves can be superimposed to obtain an interference pattern:

$$\begin{aligned} A = 2A_o \cos[\tfrac{1}{2}(k_1 x_1 - k_2 x_2 + \varphi)] \\ \cos[\omega t + \frac{\varphi}{2} - \frac{k_1 x_1 + k_2 x_2}{2}] \quad . \end{aligned} \tag{A2}$$

At the j^{th} node in the interference pattern, the null condition is

$$\tfrac{1}{2}|k_1 x_1 - k_2 x_2 + \varphi| = (2j-1)\frac{\pi}{2} \quad . \tag{A3}$$

We assume that if φ is indeed non-zero, then it is a positive number as represented in Eqs. (A1). Equation (A3) can then be written

$$\pm \left(1 - \frac{k_2 x_2}{k_1 x_1}\right) = \frac{(2j-1)\pi - \varphi}{k_1 x_1} \quad . \tag{A4}$$

Here (+) refers to the case $k_2 x_2 < k_1 x_1$. Because the null condition is represented in terms of an absolute value, there is an ambiguity of sign. However, this is not critical. The proper sign can always be determined by other means. We adopt the (+) in Eq. (A4). When a particular node is exactly at the position of the n^{th} echo, we have

$$k_1 x_1 = (2\pi f/v_1)\cdot nt_o v_1 = 2\pi f n t_o \quad . \tag{A5}$$

Here v_1 is the velocity of sound in specimen 1; f is the frequency; and t_o is the round trip transit time. Also, from the definition of the natural velocity W, we have

$$k_2 x_2 / k_1 x_1 = W_1 / W_2 \quad . \tag{A6}$$

Combining Eqs. (A5) and (A6) with Eq. (A4) we have

$$1 - \frac{W_1}{W_2} = \frac{(2j-1)\pi - \varphi}{2\pi f t_o} \left(\frac{1}{n}\right) \quad . \tag{A7}$$

If we assume that specimen 1 is at constant temperature and specimen 2 is at a variable temperature, we obtain

$$\frac{1}{W} \left.\frac{\partial W}{\partial T}\right|_P = \frac{(2j-1)\pi - \varphi}{2\pi f t_o} \frac{\partial}{\partial T} \left(\frac{1}{n}\right) \quad . \tag{A8}$$

Here we neglect a factor W_1/W_2 which is very close to unity. We can determine $\frac{1}{W} \left.\frac{\partial W}{\partial T}\right|_P$ from the slope of a plot of (1/n) vs. the temperature difference between the two specimens. We see that a non-zero phase difference φ will affect the absolute magnitude of this slope.

Ideally, the phase angle φ should be zero because the same pulse is applied to each specimen through similar circuits. If φ is identically zero, the same temperature derivative would be obtained from measurements on all available nodes. We did not always find this to be the case. For certain measurements, we obtained different slopes using different nodes. This is illustrated in Fig. 5. The dashed line in Fig. 5 indicates the correct slope which would be measured if the phase difference φ was identically zero. When the movement with temperature of more than one node

Fig. 6. The natural velocity temperature derivative $\frac{1}{W_s}\left.\frac{\partial W}{\partial T}\right|_P$ for a C_{44} mode. The data is mistakenly analyzed as if $\varphi=0$ for nodes 2 and 3. For this experiment $\varphi = 0.47\pi$. A correct analysis including this value of φ would give the dashed line shown in the figure.

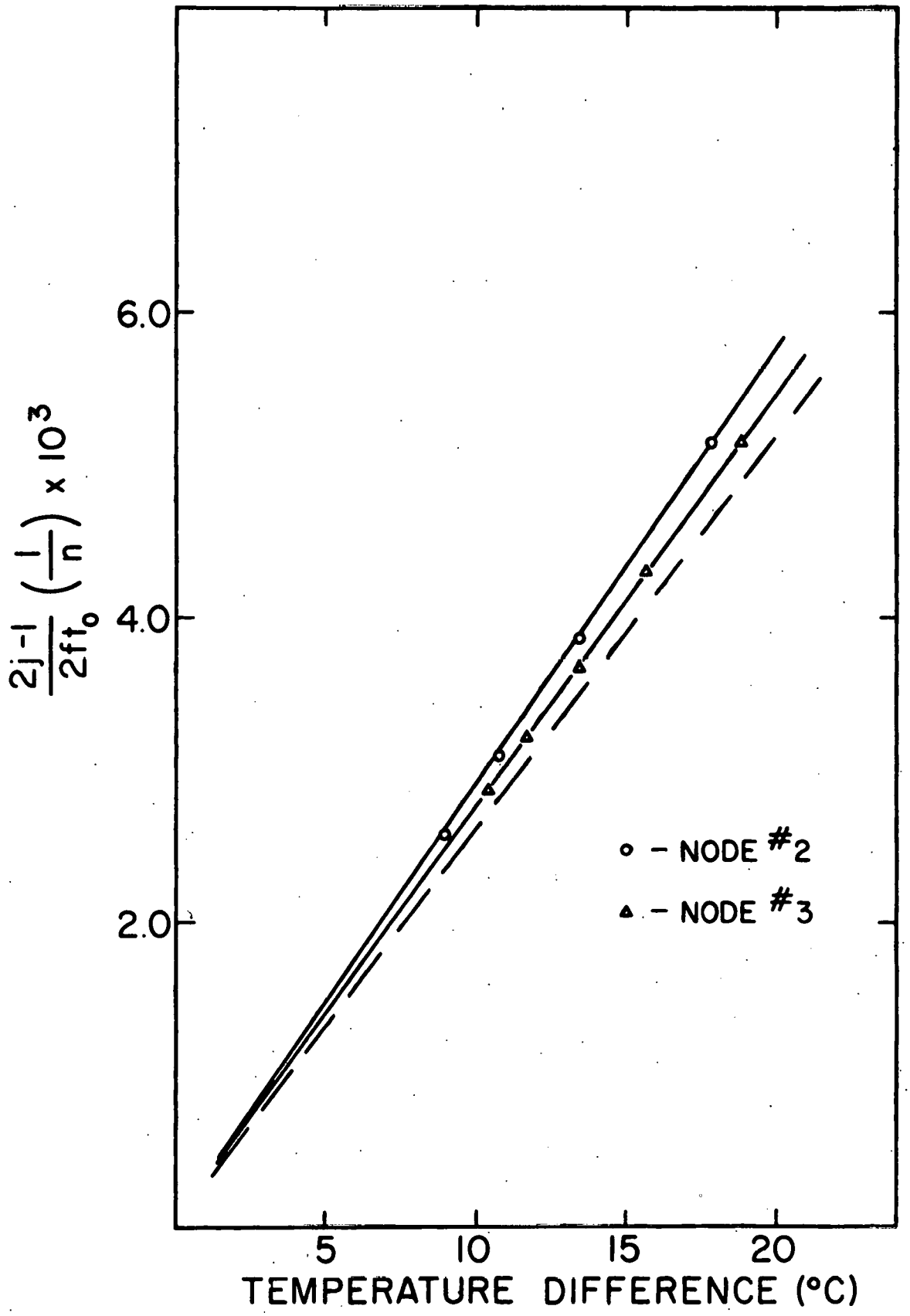
6.0
4.0
2.0
$\frac{2j-1}{2ft_o}\left(\frac{1}{n}\right) \times 10^3$
o – NODE #2
Δ – NODE #3
5
10
15
20
TEMPERATURE DIFFERENCE (°C)

was observed, it was a simple matter to determine φ and recalculate the derivative $\frac{1}{W}\left.\frac{\partial W}{\partial T}\right|_P$. This has been done for the temperature derivatives presented in Tables 2 and 3 in the text. Since the phase differences φ varied over a wide range (nearly $0 - \frac{\pi}{2}$), we believe this to be an effect due to the bond between the specimen and the quartz transducer.

APPENDIX B

The lattice energy per unit mass can be expanded in a power series in terms of the finite Lagrangian strain parameters. In tensor notation, this would be written

$$\rho_o E = \rho_o E_o + \frac{1}{2} C_{ijk\ell}\, \eta_{ij}\eta_{k\ell} + \frac{1}{6} C_{ijk\ell mn}\, \eta_{ij}\eta_{k\ell}\eta_{mn} + \cdots \qquad (B1)$$

The elastic constants are those defined by Brugger and are expressed in the full tensor notation. The linear term is not present as we are expanding about the equilibrium state.

For cubic crystals, the explicit form of the second order energy terms can be written as

$$\rho_o E_2 = \frac{1}{2} C_{11}(\eta_{11}^2+\eta_{22}^2+\eta_{33}^2) + C_{12}(\eta_{11}\eta_{22} + \eta_{22}\eta_{33}+\eta_{33}\eta_{11}) + 2C_{44}(\eta_{12}^2+\eta_{23}^2+\eta_{31}^2) . \qquad (B2)$$

Similarly, the third order term becomes

$$\rho_o E_3 = \frac{1}{6} C_{111}(\eta_{11}^3+\eta_{22}^3+\eta_{33}^3) + \frac{1}{2} C_{112}[\eta_{11}^2(\eta_{22}+\eta_{33}) + \eta_{22}^2(\eta_{33}+\eta_{11}) + \eta_{33}^2(\eta_{11}+\eta_{22})] + C_{123}(\eta_{11}\eta_{22}\eta_{33}) + 2C_{144}(\eta_{11}\eta_{23}^2+\eta_{22}\eta_{31}^2+\eta_{33}\eta_{12}^2) + 2C_{166}[\eta_{12}^2(\eta_{11}+\eta_{22}) + \eta_{23}^2(\eta_{22}+\eta_{33}) + \eta_{31}^2(\eta_{33}+\eta_{11})] + 8C_{456}(\eta_{12}\eta_{23}\eta_{31}) . \qquad (B3)$$

In Eqs. (B2) and (B3), the elastic constants are expressed in the contracted notation. Also, in these equations, equal but independent terms of the general expansion Eq. (B1) have been combined. This becomes important if we wish to differentiate the energy expressions. It must be

recognized that all nine strain tensor components η_{ij} are independent. Before differentiating, individual energy terms must be symmetrized. For example,

$$\rho_o \frac{\partial^2 E_2}{\partial \eta_{23} \partial \eta_{23}} = 2C_{44} \frac{\partial^2}{\partial \eta_{23}^2} \left(\frac{\eta_{23}+\eta_{32}}{2} \right)^2 = C_{44} . \qquad \text{(B4)}$$

APPENDIX C

Deformation (x_1): The deformation tensor is given by

$$\alpha(\nu,x_1) = \nu^{1/3} \begin{pmatrix} x_1^{1/3} & 0 & 0 \\ 0 & x_1^{1/3} & 0 \\ 0 & 0 & x_1^{-2/3} \end{pmatrix} \tag{C1}$$

The Lagrangian strain tensor (Eq. (36)) is given by

$$\eta(\nu,x_1) = \begin{pmatrix} \frac{1}{2}(\nu^{2/3}\, x_1^{2/3}-1) & 0 & 0 \\ 0 & \frac{1}{2}(\nu^{2/3}\, x_1^{2/3}-1) & 0 \\ 0 & 0 & \frac{1}{2}(\nu^{2/3}\, x_1^{-4/3}-1) \end{pmatrix} \tag{C2}$$

The unit cell of the FCC bravais lattice is described by the three vectors $\underline{a}_1 = (a/2)[0,1,1]$, $\underline{a}_2 = (a/2)[1,0,1]$, $\underline{a}_3 = (a/2)[1,1,0]$. Here a is the lattice constant. The deformed unit cell is described by the vectors

$$\begin{aligned} \underline{a}_1 &= (a/2)\ \nu^{1/3} x_1^{1/3}\ [0,1,x_1^{-1}]\ , \\ \underline{a}_2 &= (a/2)\ \nu^{1/3} x_1^{1/3}\ [1,0,x_1^{-1}]\ , \\ \underline{a}_3 &= (a/2)\ \nu^{1/3} x_1^{1/3}\ [1,1,0]\quad . \end{aligned} \tag{C3}$$

The reciprocal lattice of the FCC lattice is the BCC lattice. The deformed reciprocal lattice is described by the three vectors

$$\underline{b}_1 = (2\pi/a)\ \nu^{-1/3} x_1^{-1/3}\ [-1,1,x_1]\ ,$$

$$\underline{b}_2 = (2\pi/a)\ \nu^{-1/3} x_1^{-1/3}\ [1,-1,x_1]\ ,$$

$$b_3 = (2\pi/a)\ \nu^{-1/3} x_1^{-1/3}\ [1,1,-x_1]\ . \qquad \text{(C4)}$$

Deformation (x_2): The deformation tensor is given by

$$\alpha(\nu,x_2) = \frac{1}{3}\ \nu^{1/3}\ x_2^{1/3} \begin{pmatrix} x_2^{-1}+2 & x_2^{-1}-1 & x_2^{-1}-1 \\ x_2^{-1}-1 & x_2^{-1}+2 & x_2^{-1}-1 \\ x_2^{-1}-1 & x_2^{-1}-1 & x_2^{-1}+2 \end{pmatrix} \qquad \text{(C5)}$$

The Lagrangian strain tensor is given by

$$\eta = \frac{1}{2} \begin{pmatrix} \frac{1}{3}\ \nu^{2/3}\ x_2^{2/3}\ (x_2^{-2}+2)-1 & (21) & (21) \\ \frac{1}{3}\ \nu^{2/3}\ x_2^{2/3}\ (x_2^{-2}-1) & (11) & (21) \\ (21) & (21) & (11) \end{pmatrix} \qquad \text{(C6)}$$

The deformed unit cell is described by the vectors

$$\underline{a}_1 = (a/6)\ \nu^{1/3}\ x_2^{1/3}\ [2(x_2^{-1}-1),\ 2x_2^{-1}+1,\ 2x_2^{-1}+1]\ ,$$

$$\underline{a}_2 = (a/6)\ \nu^{1/3}\ x_2^{1/3}\ [2x_2^{-1}+1,\ 2(x_2^{-1}-1),\ 2x_2^{-1}+1]\ ,$$

$$\underline{a}_3 = (a/6)\ \nu^{1/3}\ x_2^{1/3}\ [2x_2^{-1}+1,\ 2x_2^{-1}+1,\ 2(x_2^{-1}-1)]\ . \qquad \text{(C7)}$$

The deformed reciprocal lattice is described by the vectors

$$\underline{b}_1 = (2\pi/3a)\,[x_2-4,\ x_2+2,\ x_2+2]\ ,$$

$$\underline{b}_2 = (2\pi/3a)\,[x_2+2,\ x_2-4,\ x_2+2]\ ,$$

$$\underline{b}_3 = (2\pi/3a)\,[x_2+2,\ x_2+2,\ x_2-4]\ . \qquad \text{(C8)}$$

Deformation (x_3): The deformation tensor is given by

$$\alpha(\nu,x_3) = \nu^{1/3}\ x_3^{1/3} \begin{pmatrix} \frac{1}{2}(x_3^{-1}+1) & \frac{1}{2}(x_3^{-1}-1) & 0 \\ \frac{1}{2}(x_3^{-1}-1) & \frac{1}{2}(x_3^{-1}+1) & 0 \\ 0 & 0 & 1 \end{pmatrix} \qquad \text{(C9)}$$

The Lagrangian strain tensor is given by

$$\eta = \frac{1}{2} \begin{pmatrix} \frac{1}{2}\ \nu^{2/3}\ x_3^{2/3}(x_3^{-2}+1)-1 & (21) & 0 \\ \frac{1}{2}\ \nu^{2/3}\ x_3^{2/3}(x_3^{-2}-1) & (22) & 0 \\ 0 & 0 & \nu^{2/3}\ x_3^{2/3}-1 \end{pmatrix} \qquad \text{(C10)}$$

The deformed unit cell is described by the vectors

$$\underline{a}_1 = (a/2)\ \nu^{1/3}\ x_3^{1/3}\ [\ \tfrac{1}{2}(x_3^{-1}-1),\ \tfrac{1}{2}(x_3^{-1}+1),\ 1]\ ,$$

$$\underline{a}_2 = (a/2)\ \nu^{1/3}\ x_3^{1/3}\ [\ \tfrac{1}{2}(x_3^{-1}+1),\ \tfrac{1}{2}(x_3^{-1}-1),\ 1]\ ,$$

$$\underline{a}_3 = (a/2)\ \nu^{1/3}\ x_3^{1/3}\ [x_3^{-1},\ x_3^{-1},\ 0]\ . \qquad \text{(C11)}$$

The deformed reciprocal lattice is described by the vectors

$$\underline{b}_1 = (2\pi/a)\ \nu^{-1/3}\ x_3^{-1/3}\ [-1,\ 1,\ 1]\ ,$$

$$\underline{b}_2 = (2\pi\ a)\ \nu^{-1/3}\ x_3^{-1/3}\ [1,\ -1,\ 1]\ ,$$

$$\underline{b}_3 = (2\pi\ a)\ \nu^{-1/3}\ x_3^{-1/3}\ [x_3,\ x_3,\ -1]\ . \qquad \text{(C12)}$$

REFERENCES

1. R. N. Thurston, in Physical Acoustics, edited by W. P. Mason. (Academic Press Inc., New York, 1964) Vol. IA, p. 1.

2. K. Brugger, Phys. Rev. 133, A1611 (1964).

3. Duane C. Wallace, Phys. Rev. 162, 776 (1967).

4. David Lazarus, Phys. Rev. 76, 545 (1949).

5. W. B. Daniels and Charles S. Smith, Phys. Rev. 111, 713 (1958).

6. R. E. Schmunk and Charles S. Smith, J. Phys. Chem. Solids 9, 100 (1959).

7. P. A. Smith and Charles S. Smith, J. Phys. Chem. Solids 26, 279 (1965).

8. W. B. Daniels, Phys. Rev. 119, 1246 (1960).

9. A. L. Jain, Phys. Rev. 123, 1234 (1961).

10. G. A. Alers, in Physical Acoustics, edited by W. P. Mason. (Academic Press Inc., New York, 1966) Vol. IVA, p. 277.

11. H. J. McSkimin, J. Acoust. Soc. Am. 33, 12 (1961).

12. H. J. McSkimin and P. Andreatch, J. Acoust. Soc. Am. 34, 609 (1962).

13. R. P. Espinola and P. C. Waterman, J. Appl. Phys. 29, 718 (1958).

14. Yosio Hiki and A. V. Granato, Phys. Rev. 144, 411 (1966).

15. K. D. Swartz, Thesis, University of Illinois (1966).

16. K. Salama and G. A. Alers, Phys. Rev. 161, 673 (1967).

17. R. N. Thurston and K. Brugger, Phys. Rev. 133, A1604 (1964).

18. T. L. Ochs, to be published.

19. G. N. Kamm and G. A. Alers, J. Appl. Phys. 35, 327 (1964).

20. C. S. Taylor, L. A. Willey, Dana W. Smith, and Junius D. Edwards, Metals and Alloys 9, 189 (1938).

21. T. R. Long and C. S. Smith, J. Acoust. Soc. Am. 26, 146 (1954).

22. Karl D. Swartz, J. Acoust. Soc. Am. 41, 1083 (1967).

23. Yosio Hiki, J. F. Thomas, Jr., and A. V. Granato, Phys. Rev. 153, 764 (1967).

24. G. Leibfried and W. Ludwig, Solid State Phys. 12, 275 (1961).

25. J. C. Slater, Introduction to Chemical Physics. (McGraw-Hill Book Co. Inc., New York, 1939), p. 215.

26. F. W. Sheard, Phil. Mag. 3, 1381 (1958).

27. K. Brugger, Phys. Rev. 137, A1826 (1965).

28. S. L. Quimby and P. M. Sutton, Phys. Rev. 91, 1122 (1953).

29. D. E. Schuele and Charles S. Smith, J. Phys. Chem. Solids 25, 801 (1964).

30. B. F. Figgens, G. O. Jones, and D. P. Riley, Phil. Mag. 1, 747 (1956).

31. W. F. Guiauque and P. F. Meads, J. Am. Chem. Soc. 63, 1897 (1941).

32. J. H. O. Varley, Proc. Roy. Soc. (London) A238, 413 (1956).

33. J. G. Collins and G. K. White, in Progress in Low Temperature Physics, edited by C. J. Gorter. (North Holland Publishing Co., Amsterdam, 1964).

34. N. E. Phillips, Phys. Rev. 114, 676 (1959).

35. J. G. Collins, Phil. Mag. 8, 323 (1963).

36. T. H. K. Barron, Phil. Mag. 46, 720 (1955).

37. R. H. Carr, R. D. McGammon, and G. K. White, Proc. Roy. Soc. (London) A280, 72 (1964).

38. P. B. Ghate, Phys. Rev. 139, A1666 (1965).

39. P. N. Keating, Phys. Rev. 149, 674 (1966).

40. K. Fuchs, Proc. Roy. Soc. (London) A153, 622 (1936).

41. K. Fuchs, Proc. Roy. Soc. (London) A157, 444 (1936).

42. H. B. Huntington, Solid State Phys. 7, 213 (1958).

43. R. S. Leigh, Phil. Mag. 42, 139 (1951).

44. H. Jones, Phil. Mag. 43, 105 (1952).

45. John R. Reitz and Charles S. Smith, Phys. Rev. 104, 1253 (1956).

46. J. G. Collins, Phys. Rev. 155, 663 (1967).

47. C. S. G. Cousins, Proc. Phys. Soc. (London) 91, 235 (1967).

48. F. D. Murnaghan, Finite Deformation of an Elastic Solid. (John Wiley and Sons, New York, 1951).

49. E. Wigner and F. Seitz, Phys. Rev. 43, 804 (1933).

50. E. Wigner and F. Seitz, Phys. Rev. 46, 509 (1934).

51. H. Jones, Physica 15, 13 (1949).

52. Walter A. Harrison, Phys. Rev. 116, 555 (1959).

53. N. W. Ashcroft, Phil. Mag. 8, 2055 (1963).

54. Peter J. Melz, Phys. Rev. 152, 540 (1966).

55. J. C. Phillips and L. Kleinman, Phys. Rev. 116, 287, 880 (1959).

56. V. Heine and D. Weaire, Phys. Rev. 152, 603 (1966).

VITA

Joseph Francis Thomas, Jr. was [redacted]. He received his secondary education at New Trier Township High School, Winnetka, Illinois. He attended Cornell University, Ithaca, New York, receiving the degree of Bachelor of Engineering Physics in June, 1963. Since the fall of 1963 he has been a graduate student in the Department of Physics, University of Illinois, Urbana. He received the Master of Science degree in physics in February, 1965. The author is a member of Tau Beta Pi and The American Physical Society.